IARC MONOGRAPHS

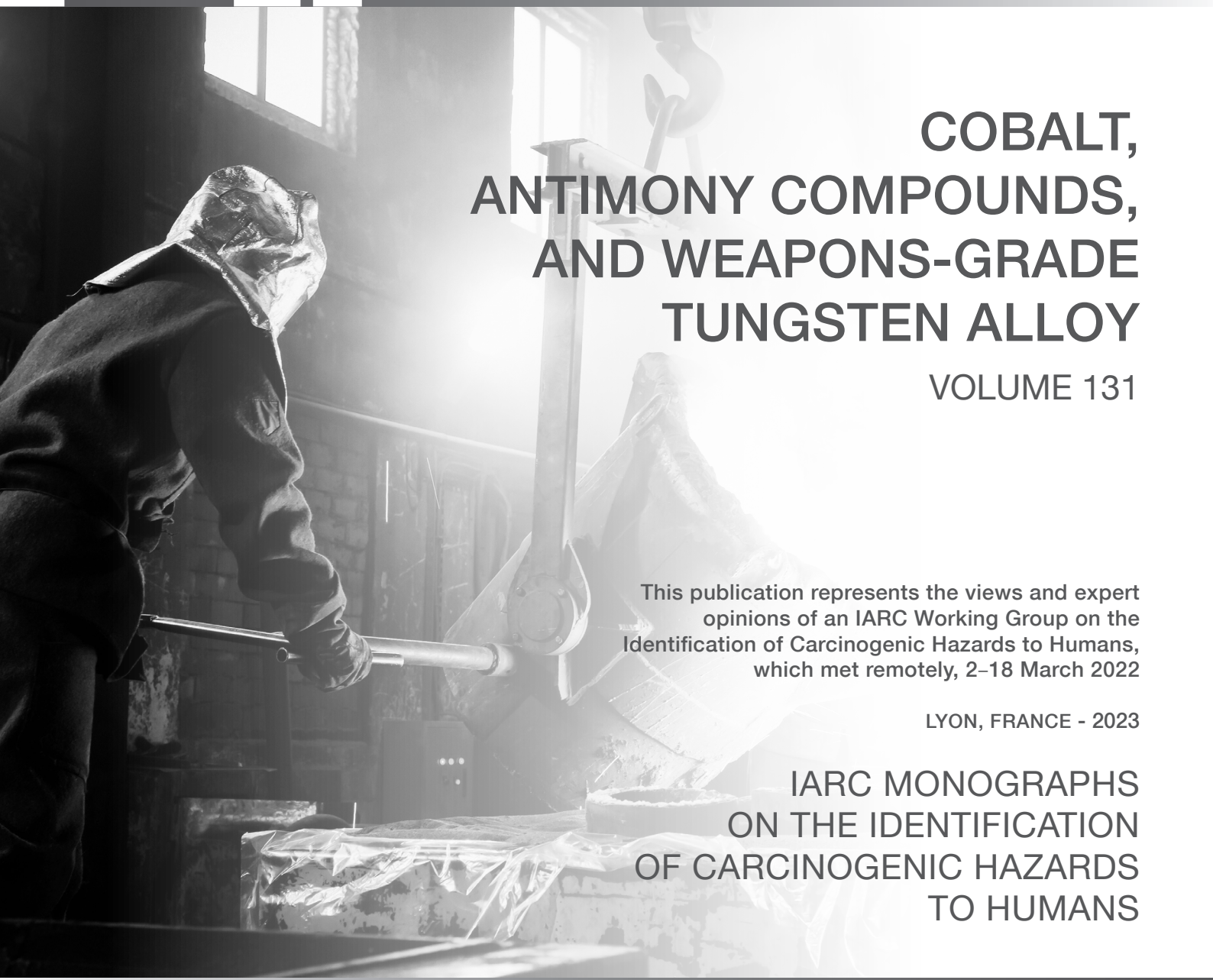

COBALT, ANTIMONY COMPOUNDS, AND WEAPONS-GRADE TUNGSTEN ALLOY

VOLUME 131

This publication represents the views and expert opinions of an IARC Working Group on the Identification of Carcinogenic Hazards to Humans, which met remotely, 2–18 March 2022

LYON, FRANCE - 2023

IARC MONOGRAPHS ON THE IDENTIFICATION OF CARCINOGENIC HAZARDS TO HUMANS

International Agency for Research on Cancer

World Health Organization

WEAPONS-GRADE TUNGSTEN (WITH NICKEL AND COBALT) ALLOY

1. Exposure Characterization

1.1 Identification of the agent

This monograph focuses on alloys containing tungsten, nickel, and cobalt that are used in the production of military weapons. Such alloys typically contain approximately 91–93% tungsten, 3–5% nickel, and 2–4% cobalt (Andrew et al., 1991, as cited in Miller et al., 2004), and are sometimes referred to as "tungsten heavy alloys" or "weapons-grade tungsten alloys". Other sources have defined these alloys more broadly in terms of the percentages of the constituent metals (tungsten, nickel, and cobalt). The Working Group defined the name of the agent under evaluation in the present monograph as "weapons-grade tungsten (with nickel and cobalt) alloy" (WGTA). [The Working Group noted that, by definition, co-exposure to tungsten, nickel, and cobalt is a feature of exposure to this agent; however, as there are limited data available for the WGTAs, exposure details for the individual elements contained in the alloys are presented when considered relevant.]

Tungsten, a relatively rare metal, has several unique chemical and physical properties that make it suitable for use in lighting, aerospace, electronic, radiation shielding, and military applications. These properties include a high density (19.3 g/mL), high melting point (3410 °C, the highest melting point of all metals), low vapour pressure, high tensile strength at temperatures greater than 1650 °C, and high corrosion resistance (US EPA, 2017; Wasel & Freeman, 2018; Michaux, 2021). It is also a good conductor of electricity (Wasel & Freeman, 2018) and has the lowest coefficient of expansion of all the metals (van der Voet et al., 2007). However, one drawback to tungsten is its low ductility (or brittleness) at room temperature; therefore, it is often combined with other elements to create alloys that have the physical and chemical properties needed for various applications (Vergara et al., 2016).

In general, tungsten alloys (including tungsten heavy alloys) are only slightly less dense than pure tungsten (16–18 g/mL compared with 19.3 g/mL). They also have high tensile strengths (1000–1700 MPa) and ductility (10–30%), and are easily machinable (Upadhyaya, 2001). Tungsten heavy alloys that are used in many military applications typically contain 90–98% tungsten by weight, with two or more transition metals such as nickel, iron, copper, and/or cobalt (van der Voet et al., 2007). The use of iron in place of cobalt enhances the ductility and strength of the alloy (van der Voet et al., 2007; Dinçer et al., 2015). One commercially available WGTA contains 91.1% tungsten, 6% nickel, and 2.9% cobalt (Kalinich et al., 2005). [The Working Group acknowledged the lack of information on

the physical and chemical properties of specific WGTAs in the literature.]

1.2 Production and use

1.2.1 Production processes and volumes

WGTAs are typically produced using the liquid-phase sintering method. In this process, elemental powders of tungsten, nickel, and cobalt are blended, isostatically compressed into desired shapes, and then sintered at high temperatures (~1500 °C) under a protective atmosphere. The sintering temperatures are lower than the melting point of tungsten, but higher than the melting points of the alloying metals. To prevent intermetallic compounds, such as WCo_3, from forming, post-sintering water quenching is performed (Upadhyaya, 2001; Ogundipe et al., 2006). The composite that is formed contains two phases: a tungsten phase, which consists of almost-pure tungsten grains approximately 30–35 μm in size, and a binder phase, which surrounds the tungsten phase and contains dissolved tungsten in a matrix of nickel and cobalt (Ogundipe et al., 2006; Sunwoo et al., 2006). The quantities and compositions of the alloying metals determine the amount of tungsten present in the binder phase (Ogundipe et al., 2006).

Overall, the production of WGTAs accounts for only a small proportion of the global demand for tungsten, because more than 60% of tungsten is used for the production of cemented carbides (Michaux, 2021). Tungsten alloys have been used to replace lead and depleted uranium in munitions since the 1990s (Zoroddu et al., 2018). [However, the Working Group acknowledged that details regarding the production volumes of the WGTAs and of the munitions containing them are not readily available in the published literature.] In general, the demand for tungsten is closely tied to the global economy, and global production of tungsten for use in the construction, metalworking, mining, and oil and gas industries has increased from approximately 26 000 tonnes in 1994 to 84 000 tonnes in 2020 (United States Geological Survey, 1996, 2021). China is the world leader in tungsten production, producing more than 69 000 tonnes [more than 82% of the world's production] in 2020 (United States Geological Survey, 2021), followed by Viet Nam and the Russian Federation (accounting for [5.1%] and [2.6%] of global tungsten production, respectively).

1.2.2 Uses

The search for more "environmentally friendly" alternatives to depleted uranium and lead in munitions led to the investigation and use of tungsten alloys in several armour-penetrating and small-calibre munitions during the 1990s (Zoroddu et al., 2018). At the time, given the limited data available, tungsten was considered relatively inert; therefore, it was perceived to be less environmentally toxic than depleted uranium or lead (Ogundipe et al., 2006). Tungsten–nylon munitions largely replaced the use of lead bullets in the USA from 1999 until concerns about flight instability affecting munition performance halted their production in 2003 (Clausen & Korte, 2009). However, only the WGTAs were deemed to be suitable replacements for depleted uranium in kinetic energy penetrators. Designed to pierce armour, these munitions do not explode, but instead are propelled at high speeds and rely on their mass to penetrate, damage, and destroy enemy targets (Machado, 2011). Therefore, with densities similar to depleted uranium and desirable mechanical properties, WGTAs were used by the militaries of many nations to replace depleted uranium in kinetic energy penetrators, guided missiles, and other types of armour-piercing munitions (Kalinich et al., 2005, 2008; van der Voet et al., 2007; Dinçer et al., 2015). [The Working Group acknowledged that information on the use of munitions containing WGTAs by

specific countries is lacking. In addition, other non-munition-related uses for the WGTAs were not available to the Working Group.]

1.3 Detection and quantification

1.3.1 Air

Exposure monitoring of WGTAs in air is achieved by measuring air concentrations of each individual element: tungsten, nickel, and cobalt. Table 1.1 summarizes examples of analytical methods used for the measurement of tungsten and nickel. For details on the measurement of cobalt in air, refer to Table 1.5 in the monograph on Cobalt metal (without tungsten carbide) and some cobalt compounds, in the present volume.

The recommended technique of the United States National Institute for Occupational Safety and Health (NIOSH), Method No. 7074, for the measurement of tungsten in air uses flame atomic absorption spectrometry (AAS). This method involves the collection of air samples using cellulose ester filters followed by acid digestion, and has analytical limits of detection (LODs) of 50 and 125 µg for soluble and insoluble forms of tungsten per sample, respectively (ATSDR, 2005a).

As described in United States Occupational Safety and Health Administration (OSHA) Method ID-213, air concentrations of tungsten can also be measured using inductively coupled plasma-atomic emission spectroscopy (ICP-AES) (OSHA, 1994). Before ICP-AES analyses, samples are collected using mixed cellulose ester filters and subjected to acidification. This method has an LOD of 0.34 mg/m^3 (US EPA, 2017).

Common methods for the measurement of nickel and cobalt in air samples include flame or graphite furnace AAS, ICP-AES, and inductively coupled plasma mass spectrometry (ICP-MS) (ATSDR, 2004, 2005b). Samples are typically collected on glass or quartz fibre filters and undergo acid or microwave-assisted digestion (US EPA, 1999d). For both nickel and cobalt, reported LODs are lower for methods using graphite furnace AAS and ICP-MS than for flame AAS and ICP-AES. As shown in Table 1.1, reported sample LODs for nickel range from 0.02 ng/m^3 using ICP-MS (US EPA, 1999c) to 3.1 ng/m^3 using ICP-AES. For cobalt, reported LODs range from 0.01 ng/m^3 using ICP-MS (US EPA, 1999c) to 2.2 µg/m^3 using flame AAS (US EPA, 1999a).

The presence of WGTA particles in air can be determined using scanning electron microscopy with energy-dispersive X-ray analysis (SEM-EDXA), energy-dispersive X-ray fluorescence, and laser ablation inductively coupled plasma mass spectrometry (LA-ICP-MS). These methods are described further in Section 1.3.4 of the present monograph.

1.3.2 Water

Exposure monitoring for WGTAs in water is also achieved by measuring concentrations of each individual element: tungsten, nickel, and cobalt. For analytical methods for tungsten and nickel measurement, see Table 1.1 in the present monograph, and for analytical methods for cobalt measurement, see Table 1.5 in the monograph on Cobalt metal (without tungsten carbide) and some cobalt compounds, in the present volume.

The most sensitive analytical method for the measurement of concentrations of metals in water is ICP-MS. ICP-MS is a multi-element analytical technique, which typically requires the filtration and acidification of samples before analysis and offers LODs in the sub or low parts-per-billion range for most metals (US EPA, 2014). Specifically, LODs for tungsten are 0.4–5 µg/L, depending on the species being studied (Bednar et al., 2007), and LODs as low as 0.5 µg/L have been reported for nickel (ATSDR, 2005b).

Table 1.1 Representative methods for the detection and quantification of tungsten and nickel

Sample matrix	Sample preparation (method)	Analytical technique (method)	LOD	Reference
Tungsten				
Air	Collection on cellulose ester membrane filter, acid digestion, drying, addition of sodium hydroxide and sodium sulfate, and dilution	Flame AAS (NIOSH Method 7074)	Soluble tungsten, 50 µg; insoluble tungsten, 125 µg	ATSDR (2005a) NIOSH (1994a)
Air	Collection on mixed-cellulose ester filter and acidification	ICP-AES (OSHA Method ID-213)	0.34 mg/m^3	US EPA (2017) OSHA (1994)
Water	Filtration and acid digestion using US EPA SW-846 Method 3050 (modified)	ICP-MS	NR	Clausen & Korte (2009)
Water	Filtration and acid digestion	High-performance liquid chromatography ICP-MS (SW-846 US EPA Method 6020B, modified)	0.1–5 µg/L, depending on the species	Bednar et al. (2007)
Soil	Microwave-assisted acid digestion using modified version of US EPA SW-846 Method 3051A	ICP-MS (SW-846 US EPA Method 6020B, modified)	NR	Clausen & Korte (2009)
Urine	Dilution and acidification	ICP-MS with dynamic cell reaction technology	0.018 µg/L	CDC (2019)
Urine	Dilution and acidification	ICP-AES (NIOSH Method 8310)	50 µg/L	ATSDR (2005a) NIOSH (1994b)
Blood	Samples typically wet ashed with nitric acid and then diluted	ICP-MS	Plasma, 0.01 µg/L; serum, 0.04 µg/L; and blood, 0.2 µg/L	ATSDR (2005a)
Nickel				
Air	Collection on glass or quartz fibre filter, acid or microwave digestion; microwave preferred	AAS (US EPA Methods IO-3.1 and IO-3.2)	1.1 ng/m^3 using flame AAS, 0.1 ng/m^3 using graphite furnace AAS	ATSDR (2005b) US EPA (1999a)
Air	Collection on glass or quartz fibre filter, hot acid or microwave digestion (US EPA Method IO-3.1)	ICP-AES (US EPA Method IO-3.4)	3.1 ng/m^3	ATSDR (2005b) US EPA (1999b)
Air	Collection on glass or quartz fibre filter; microwave or hot acid digestion (US EPA Method IO-3.1)	ICP-MS (US EPA Method IO-3.5)	0.02 ng/m^3	ATSDR (2005b) US EPA (1999c)
Water	Filtration and acid digestion	ICP-MS (US EPA Method 200.8)	0.5 µg/L	ATSDR (2005b) US EPA (1994)
Water	Filtration and acid digestion	ICP-MS (US EPA Method 6020B)	[NR, but generally < 0.1 µg/L for metals]	US EPA (2014)

Table 1.1 (continued)

Sample matrix	Sample preparation (method)	Analytical technique (method)	LOD	Reference
Soil	Microwave-assisted acid digestion and filtration (US EPA SW-846 Method 3051A)	ICP-MS (US EPA Method 6020B)	[NR, but generally < 0.1 µg/L for metals]	US EPA (2014)
Urine	Dilution and acidification	ICP-MS	0.31 µg/L	CDC (2018)
Blood	Acid digestion using mixture of nitric, perchloric, and sulfuric acids	ICP-AES (NIOSH 8005)	1 µg/100 g of blood	NIOSH (1994c) ATSDR (2005b)

AAS, atomic absorption spectroscopy; ICP-AES, inductively coupled plasma-atomic emission spectroscopy; ICP-MS, inductively coupled plasma mass spectrometry; LOD, limit of detection; NIOSH, National Institute for Occupational Safety and Health; NR, not reported; OSHA, Occupational Safety and Health Administration; US EPA, United States Environmental Protection Agency.

1.3.3 Soil

As shown in Table 1.1 and in Table 1.5 in the monograph on Cobalt metal (without tungsten carbide) and some cobalt compounds, in the present volume, concentrations of tungsten, nickel, and cobalt, in the sub and low parts-per-billion range, have also been measured in soil using ICP-MS (US EPA, 2014). Collected soil samples are typically prepared for analysis using microwave-assisted acid digestion (US EPA, 2007). For tungsten, modifications to the standard United States Environmental Protection Agency (US EPA) soil preparation protocol are required to maintain tungsten in a soluble form. These modifications include the addition of phosphoric acid to the digestion process and changes to the rinse solution (Clausen & Korte, 2009). Samples are then filtered and analysed using ICP-MS (US EPA, 2014).

1.3.4 Munitions fragments

There are currently no analytical methods that can be used to determine the composition of embedded metal fragments in the body. However, the composition of surgically excised metal fragments from war-related injuries can be determined using a variety of different analytical techniques, including SEM-EDXA, energy-dispersive X-ray fluorescence, and LA-ICP-MS (Centeno et al., 2014). SEM-EDXA can be used to define the elemental compositions and physical appearances of metal fragments, and energy-dispersive X-ray fluorescence is a non-destructive technique that permits qualitative and semi-quantitative elemental analysis of a fragment's surface. LA-ICP-MS allows for semiquantitative elemental composition analysis of the entire fragment, without requiring digestion of the specimen (Centeno et al., 2014).

1.3.5 Human biomarkers

There are no biomarkers of human exposure that are specific to WGTAs. However, concentrations of tungsten, nickel, and cobalt can each be measured in biological samples, including blood and urine, using ICP-MS; for tungsten and nickel, see Table 1.1, and for cobalt, see Table 1.6 in the monograph on Cobalt metal (without tungsten carbide) and some cobalt compounds, in the present volume. In biological monitoring programmes and large population studies, urine is often the preferred matrix because sample collection is easy and non-invasive (Smolders et al., 2009). Analysis of urine typically involves dilution of the sample in 2% nitric acid, and detection limits range from 0.1 to 1 ppb for most metals (Centeno et al., 2014). For example, detection limits in urine as low as 0.018, 0.31, and 0.023 µg/L for tungsten, nickel, and cobalt, respectively, have been reported (CDC, 2018, 2019).

To assess the distribution of solubilized metals in soft tissue after the removal of a metal fragment from a war-related injury, candidate methodologies including SEM-EDXA, X-ray photoelectron spectroscopy, and LA-ICP-MS have been investigated (Centeno et al., 2014; Smith et al., 2021). However, a recent study comparing these methods suggested that LA-ICP-MS is the only method that is sufficiently sensitive to detect trace elements in tissue samples (Smith et al., 2021).

1.4 Occurrence and exposure

1.4.1 Environmental occurrence

WGTAs do not occur naturally in the environment. No data on environmental exposures that may occur from the production and use of WGTAs in military weapons were available to the Working Group. However, studies measuring concentrations of tungsten, nickel, and cobalt

in the environment resulting from hard-metal production and the deposition of metal particles in soil resulting from the firing of other tungsten-containing munitions can provide some insight into potential environmental exposure pathways.

In general, background concentrations of tungsten in soil are relatively low, being reported to average around 1 mg/kg (Zoroddu et al., 2018), and tungsten is not detected in most ground and surface waters (ATSDR, 2005a). However, elevated concentrations of tungsten, as well as cobalt, have been found in soil and water samples in communities surrounding hard-metal industries where tungsten and cobalt powders have been used. For example, Fallon (Nevada), USA, is a community known to have elevated background surface dust concentrations of tungsten and cobalt [< 10 and 15 mg/kg, respectively]. Spatial patterns and high peak concentrations of tungsten and cobalt [934 and 98 mg/kg, respectively] measured in environmental surface dust samples from the surrounding community have suggested the local hard-metal industry to be the point source (Sheppard et al., 2007). [The Working Group considered that although the local hard-metal industry was primarily involved in the production of tungsten carbides and not the WGTAs in question, these findings suggest that air, soil, and groundwater contamination may occur in communities surrounding hard-metal industries that produce tungsten alloys.]

Elevated tungsten concentrations, orders of magnitude higher than background levels, have also been found in soil and groundwater samples from military firing ranges (Clausen & Korte, 2009; Bostick et al., 2018). For example, studies have found tungsten concentrations in soil to be as high as 2080 mg/kg (Clausen & Korte, 2009) and 5500 mg/kg (Bostick et al., 2018). Although tungsten concentrations decrease rapidly with increasing soil depth, elevated tungsten concentrations have also been detected in pore-water samples collected from lysimeters installed in berm areas, and in groundwater well samples collected 30 feet below the surface, at concentrations ranging from 0.001–400 to 0.001–0.56 mg/L, respectively (Clausen & Korte, 2009). In comparison, background tungsten concentrations in surface water samples were reported to be below the detection limit of 0.0002 mg/L. However, these studies were conducted at military firing ranges for small arms where tungsten–nylon munitions were primarily used. [The Working Group acknowledged that soil and water tungsten concentrations related to firing of WGTA munitions would probably differ. Although these studies may not be representative of all settings in which the agent could be released, they have shed light on the environmental fate of tungsten deposited in soil, showing that over time (and especially in areas with high acidity) tungsten in soil can solubilize and migrate into groundwater.] Additional research suggests that tungsten deposited in soil rapidly oxidizes to hexavalent tungsten(VI) species, the majority being polytungstates and/or polyoxometalates (Bostick et al., 2018). Polyoxometalates are considered to be weakly retained in soil, thereby increasing tungsten's mobility and solubility in the environment, and potentially leading to long-range transport of tungsten in the soil and subsequent groundwater contamination (Bostick et al., 2018).

1.4.2 Occupational exposure

The main route of occupational exposure to metals contained in WGTAs is via the respiratory tract. Exposure to metal particulates and aerosols via inhalation can occur during the production or firing, or result from the impact, of military munitions that contain the agent. In addition, it is possible that service members injured as a result of the impact of WGTA munitions may experience ongoing systemic metal exposure because of retained WGTA fragments in tissue.

(a) Exposure via inhalation

There are no published studies specifically examining exposure to the agent among workers who are involved in the production of WGTAs. However, several studies have investigated tungsten, nickel, and cobalt exposure in workers involved in the production of tungsten carbides (Kennedy et al., 2017; Westberg et al., 2017). The manufacturing process for tungsten carbides is similar to that for WGTAs as it involves the blending, pressing, forming, and sintering of metal powders. A study in Sweden reviewed historical personal and area air concentrations of tungsten, nickel, and cobalt for workers producing primarily tungsten carbides from 1970 to 2012 (Westberg et al., 2017). Area air concentrations of tungsten were not clearly reported, but area air concentrations of cobalt and nickel ranged from 0.0001 to 2.8 mg/m^3 (Westberg et al., 2017). Workers involved in pressing and powder and roll production had the highest metal exposure. [The Working Group noted that these findings are from tungsten-carbide production facilities and that exposure concentrations related to the production of WGTAs probably differ.]

Inhalation exposure of military personnel to aerosols of metals can result from the firing and resulting impact of WGTAs into targets. An exposure study conducted by the United States Army Research Laboratory measured concentrations of metal aerosols in the breathing zones of range personnel. Two experiments involving 120 mm KEW-A2 penetrators, containing WGTA, being fired against steel plates were conducted each day over a 6-day period (Gunasekar & Stanek, 2011). Although specific metal aerosol concentrations were not published, metal aerosol concentrations in the personal breathing zones of range personnel were reported to be 10 times lower than established threshold limit values during a 9-hour work shift. [However, the Working Group noted that these aerosol concentrations were measured in a controlled study environment that had existing engineering controls (i.e. proper ventilation), and it is unclear whether such engineering controls would be feasible in a combat situation.]

The firing of WGTA munitions that are used to perforate armoured vehicles can also result in the aerosolization of fine metal particles upon impact. When kinetic energy penetrators perforate a target, aerosol debris is generated at the front and rear of the target because of target and rod erosion (Machado, 2011). In a simulation experiment, Gold et al. (2007) used gravimetric analyses and scanning electron microscopy to assess potential exposure to aerosolized metal particulates of crew members riding in an Abrams tank breached by a kinetic energy penetrator containing WGTA. Although specific concentrations of tungsten, nickel, and cobalt in breathing zone air samples were not reported, the initial total concentrations of inhalable aerosols (can be breathed into the nose or mouth) and respirable aerosols (can penetrate beyond the terminal bronchioles into the gas–exchange region of the lungs) measured in the crew compartment were 6–12 and 5 g/m^3, respectively. At the end of the 2-hour test period, concentrations were in the milligrams-per-cubic-metre range. [The Working Group noted that similar aerosol concentrations may be found in combat situations, especially if vehicle ventilation systems fail, but that it is unclear how often such a scenario would occur.]

Machado et al. (2010) conducted a similar experiment, passing a subscale kinetic energy penetrator containing WGTA through steel plates in an encapsulated environment to characterize the aerosol particulates produced, and assess the probable resulting respiratory and inflammatory health effects. Particulate specimens, captured using cascade impactors, were analysed using gravimetric methods to determine total particulate weights and concentrations, while inductively coupled plasma optical emission spectrometry was used to assess the respirable

concentrations of each metal. Most of the aerosol generated consisted of nano-sized particles (with a size ranging from 1 to 100 nm), with overall total and total respirable particulate concentrations of 116 and 80 mg/m^3, respectively. Iron from the steel plates was found to be predominant in the air samples, with concentrations of 51.90 and 40.20 mg/m^3 for total and respirable particulates, respectively. Total and respirable particulate concentrations were 3.7 and 1.9 mg/m^3 for tungsten, 0.741 and 0.537 mg/m^3 for nickel, and 0.415 and 0.415 mg/m^3 for cobalt.

(b) Fragment-related exposures

Individuals with war-related injuries may have embedded fragments containing WGTAs in tissue, resulting in long-term exposure to metal ions from the retained fragments. Estimates suggest that more than 40 000 United States military veterans may have an embedded fragment injury; however, most of these injuries are reported to be from contact with improvised explosive devices (Gaitens et al., 2017). The number of embedded-fragment injuries related specifically to WGTA munitions is unknown, but such injuries are considered to be relatively rare, because no published reports were available relating to removal of WGTA fragments from an individual.

As a result of toxicity concerns related to the use of WGTAs, a United States Department of Defense policy in 2007 mandated that all surgically removed fragments must be sent for laboratory analysis (Centeno et al., 2014; Kalinich & Kasper, 2016). Quantitative chemical analyses of more than 800 fragments surgically removed from 344 United States military personnel over a 6-year period revealed that only one fragment contained tungsten (Centeno et al., 2014). This fragment also contained trace concentrations of lead and titanium, but no detectable concentrations of nickel or cobalt. SEM-EDXA analysis of adherent tissue accompanying the fragment showed the presence of single tungsten particles, with a size range of 1–2.5 µm, that were non-uniformly distributed throughout the tissue. (Centeno et al., 2014). [The Working Group noted that the availability and use of WGTA munitions varies among countries and therefore WGTA exposures in wounded United States military veterans may not be representative of other military populations.]

Most embedded fragments (often multiple) from war-related injuries are not excised because of the risk of surgical morbidity (Centeno et al., 2014; Gaitens et al., 2016, 2017). Therefore, on the basis of evidence from animal and human studies, which suggests that metal ions can be released from retained fragments over time, permitting their entry into the systemic circulation, biomonitoring of metal concentrations in urine has been used to gain insight into fragment-related exposures (Gaitens et al., 2016, 2017). In a study of more than 500 United States military veterans who reported having embedded fragments from war-related injuries, urine concentrations of 14 different metals frequently found in fragments were measured using ICP-MS (Gaitens et al., 2017). Results were reported as micrograms of metal per gram of creatinine (µg/g creatinine) and compared with reference values from unexposed populations. Among veterans, mean concentrations in the urine were reported to be 0.23 µg/g creatinine (range, 0.003–2.70) for tungsten, 2.42 µg/g creatinine (range, 0.02–76.25) for nickel, and 0.58 µg/g creatinine (range, 0.07–22.31) for cobalt. While urinary concentrations of tungsten, nickel, and cobalt were higher than the established reference values in approximately 12%, 5%, and 9% of samples, respectively, these elevations could not be directly attributed to the presence of a WGTA fragment, as other potential sources of metal exposure must be considered. The composition of a fragment can only be confirmed if it is removed and analysed.

1.4.3 Exposure of the general population

The general population is not likely to be exposed to WGTAs except when living in close proximity to locations where WGTA munitions are manufactured or have been fired. [However, the Working Group acknowledged that there was a lack of available data to enable the characterization of exposure to the agent.]

1.5 Regulations and guidelines

In 2007, a memorandum from the United States Secretary of Defense encouraged munition developers and researchers to consider using alternative materials to WGTAs in munitions production (Magness et al., 2014). The memorandum was written after the results of a study in rats showed rapid development of rhabdomyosarcomas in rats implanted with WGTA pellets (Kalinich et al., 2005). However, to date, there are no known bans, in the USA or elsewhere, on the use of WGTAs in military munitions.

There are no health and safety regulations or guidelines specific to WGTAs, although they do exist for the specific elements that they contain. [The Working Group noted that regulations and guidelines for tungsten, nickel, and cobalt are limited in applicability since they are not specific to WGTAs; however, in the absence of specific regulations and guidelines for WGTAs, they may provide useful information.] Table 1.2 and Table 1.3 summarize guidelines and regulatory limit values for tungsten and nickel. Guidelines and regulatory limit values for cobalt are described in Section 1.5 and occupational exposure limits in some countries are summarized in Table S1.15 in the monograph on Cobalt metal (without tungsten carbide) and some cobalt compounds in the present volume.

1.6 Quality of exposure assessment in key epidemiological studies of cancer and mechanistic studies in humans

1.6.1 Epidemiological studies of cancer in humans

No epidemiological studies of cancer in humans exposed to WGTAs were available to the Working Group.

1.6.2 Mechanistic studies in humans

(a) Exposure assessment methods

The Working Group identified one mechanistic study for which a critical appraisal of exposure assessment methods was undertaken (De Hauteclocque et al., 2002; see also Table S1.4; Annex 1, Supplementary material for Section 1, Exposure Characterization, web only, available from: https://publications.iarc.fr/618).

In a case report of a single hard-metal industry worker who developed asthma, De Hauteclocque et al. (2002) assessed exposure to tungsten and other metals using occupational history and bronchoalveolar lavage (BAL) fluid. Urinary concentrations of nickel and cobalt, but not tungsten, were also measured.

(b) Critical review of exposure assessment

Urine is not always a preferred medium for the assessment of internal concentrations of metals (e.g. lead), and the exact period of exposure indicated by the urine sample depends on the biological half-life of the metal being investigated.

The case report by De Hauteclocque et al. (2002) provided a detailed, qualitative narrative history for exposure to hard metal dust. This exposure included tungsten carbide, which is not the agent evaluated in the present monograph. The case report did not clearly describe whether the worker was exposed to WGTAs. Biological measurements of tungsten were conducted after

Table 1.2 Occupational exposure limits for tungsten in different countries

Countries	Limit values (mg/m³)			
	Soluble tungsten and its compounds		Insoluble tungsten and its compounds	
	8-hour	Short-term	8-hour	Short-term
Austria[a], Denmark	1	2	5	10
Australia, Belgium[b], Canada (Ontario), Canada (Quebec), Ireland[c], Republic of Korea, Spain, USA – NIOSH[b], United Kingdom	1	3	5	10
New Zealand	1	–	5	10
Finland, Israel[d], Poland, Singapore, Switzerland[c]	1	–	5	–
Sweden	5	–	5	–
China[b]	–	–	5	10
Norway, USA – OSHA[e]	–	–	5	–

NIOSH, National Institute for Occupation Safety and Health; OSHA, Occupational Safety and Health Administration.

[a] Values for inhalable aerosol.

[b] 15-minute averages for short-term limit values.

[c] 15-minute reference period for short-term limit values.

[d] Values for inhalable fraction.

[e] For construction and maritime industries only (OSHA, 2021).

Adapted from IFA (2022a).

Table 1.3 Occupational exposure limits for nickel and nickel compounds in different countries

Countries	Limit values (mg/m³)									
	Nickel, metal		Nickel, metal, total dust		Nickel, metal and compounds		Nickel compounds, insoluble		Nickel compounds, soluble	
	8-hour	Short-term	8-hour	Short-term	8-hour	Short-term	8-hour	Short-term	8-hour	Short-term
Australia, Canada (Ontario)[a], China, France, Republic of Korea, Singapore, Spain, USA – OSHA	–	–	1	–	–	–	–	–	–	–
Ireland, Sweden, Switzerland[a]	–	–	0.5	–	–	–	–	–	–	–
Austria	–	–	0.5	2	–	–	–	–	–	–
Belgium	1	–	1	–	–	–	–	–	–	–
Canada (Quebec)	1	–	1	–	–	–	1	–	0.1	–
Denmark	–	–	0.05	0.1			0.01	0.02[b]	0.05	0.1[b]
Finland[c]	0.01	–	–	–	–	–	–	–	–	–
Germany	0.006[d,e]	0.048[b,d,e]	–	–	0.03[d]	0.24[b,d]	–	–	–	–
Hungary	–	–	0.1	0.1	–	–	–	–	–	–
Israel	1.5	–	–	–	–	–	0.2	–	0.1	–
Japan	1	–	–	–	–	–	0.1[f]	–	0.01	–
Latvia	–	–	0.05	–	–	–	–	–	–	–
New Zealand[d]	–	–	0.005	–	–	–	–	–	–	–
Norway	–	–	–	–	0.05	–				
Romania[b]	–	–	–	–	0.1	0.5	–	–	–	–
USA – NIOSH	–	–	0.015	–	–	–	–	–	–	–

NIOSH, National Institute for Occupation Safety and Health; OSHA, Occupational Safety and Health Administration.

[a] Values for inhalable aerosol.

[b] 15-minute average for short-term limit values.

[c] Calculated as nickel.

[d] Values for respirable fraction.

[e] An assessment based on the occupational exposure limit for nickel metal can be made if only metal is present.

[f] Values for total dust as nickel.

Adapted from IFA (2022b).

onset of the outcome. Co-exposure to cobalt, chromium, and nickel was described.

2. Cancer in Humans

No data were available to the Working Group.

3. Cancer in Experimental Animals

See Table 3.1.

3.1 Mouse

Groups of 10 or 20 male B6C3F$_1$ mice [age not reported, purchased at age 3–4 weeks] were given a single intramuscular implantation of four pellets fabricated from WGTA (91.1% tungsten, 6% nickel, and 2.9% cobalt), tantalum (negative control), or nickel (positive control) (1 mm diameter × 2 mm length, designated as groups at the higher dose), with two pellets inserted into each quadricep, and followed for up to 24 months (Emond et al., 2015a). Groups of 20 male mice were given a single implantation of two pellets of test alloy plus two pellets of tantalum per mouse and followed for 24 months (designated as groups at the lower dose). Groups of 10 or 20 male mice followed for 24 months served as surgical-sham controls. Groups of 10 mice were killed at 1, 3, 6, and 12 months (groups at the higher dose), while groups of 20 mice were killed at 24 months (at the lower and higher dose, and the surgical-sham groups). Median survival age for the groups implanted with pellets of WGTA at the lower and higher dose, nickel at the lower and higher dose, and tantalum was 92.5, 72.5, 83.5, 61.5, and 99.5 weeks, respectively. Gain of body weight (bw) of mice in the group at the higher dose of WGTA was slower than that of controls but did not become statistically significant until week 32 post-implantation. Complete necropsies and histopathological evaluations were performed.

In mice implanted with WGTA, there was a significant increase in the incidence of invasive sarcoma (identified as rhabdomyosarcoma) at sites of implantation in mice killed at 6, 12, and 24 months (in the groups at both the lower and higher dose) post-implantation [P = 0.0015, $P < 0.0001$, and $P = 0.0042$, respectively, assessed by Fisher exact test] compared with tantalum-implanted or surgical-sham controls. At 24 months, there was a significant positive trend [$P < 0.001$, Cochran–Armitage test] in the incidence of rhabdomyosarcoma for the groups implanted with WGTA. No surgical-sham controls or tantalum-implanted mice developed tumours, and all mice implanted with nickel developed rhabdomyosarcomas starting 3 months post-implantation. Neither the nickel- nor the WGTA-induced tumours metastasized to regional or distant sites.

[The Working Group noted that the duration of exposure was adequate, and that the quality of analytical techniques and statistical analyses was good. However, there was no group of mice implanted with tungsten only, statistical analysis for tumour incidence was not provided, the potential role of inflammatory components was not addressed properly (e.g. there was no investigation regarding the involvement of myofibroblasts, among other factors), and there were low numbers of mice per group.]

3.2 Rat

Four groups of 46 or 36 male Fischer 344 rats (age, 9 weeks) were implanted intramuscularly with 20 pellets (1 mm diameter × 2 mm length), split between each hind leg, of tantalum (negative control; purity, 99.95%; n = 46), WGTA (91.1% tungsten, 6.0% nickel, and 2.9% cobalt) (4 WGTA-based munitions pellets and 16 tantalum pellets in the group at the lower dose; 20 WGTA pellets in the group at the higher dose; both n = 46), or nickel (positive control; purity, 99.995% metallic

Table 3.1 Studies of carcinogenicity with weapons-grade tungsten (with nickel and cobalt) alloy in mice and rats

Study design Species, strain (sex) Age at start Duration Reference	Route Agent tested, purity Vehicle Dose(s) No. of animals at start No. of surviving animals	Tumour incidence	Significance	Comments
Full carcinogenicity Mouse, B6C3F$_1$ (M) NR (purchased at age 3–4 wk) Up to 24 mo (104 wk) Emond et al. (2015a)	Intramuscular implantation WGTA, (91.1% W, 6% Ni, and 2.9% Co) None Pellet(s): 0 (sham control) or 4 Ta (control) for 6 mo, 4 WGTA for 6 mo 0 (sham control) or 4 Ta (control) for 12 mo, 4 WGTA for 12 mo 0 (sham control) or 4 Ta (control) for 24 mo, 2 WGTA + 2 Ta for 24 mo (lower dose), 4 WGTA for 24 mo (higher dose) 1× 10, 10, 10, 10, 20, 20, 20 NR, NR, NR, NR, 10 [sham control, read from Fig. 1] or 7 [Ta control, read from Fig. 1], 5 [read from Fig. 1], 1 [read from Fig. 1]	*Implantation site:* rhabdomyosarcoma 0/10 (control, 6 mo), 7/10* (WGTA, 6 mo) 0/10 (control, 12 mo), 9/10** (WGTA, 12 mo) 0/20 (control, 24 mo)[a], 7/20*** (WGTA, lower dose, 24 mo), 16/20** (WGTA, higher dose, 24 mo)	*[$P = 0.0015$, Fisher exact test] **[$P < 0.0001$, Fisher exact test] ***[$P = 0.0042$, Fisher exact test]; versus respective sham control, [a][$P < 0.001$, Cochran–Armitage trend test]; incidence in Ta-implanted (control) mice or sham controls, and consequently statistical comparisons with WGTA-implanted groups, was identical	Principal strengths: adequate duration of study, good quality of analytical techniques, and appropriate statistical analysis, except for tumour incidence (NR) Principal limitations: small number of mice per group, lack of a group implanted with W only, lack of statistical analysis for tumour incidence, and inflammatory components were not addressed properly (e.g. no investigation of myofibroblast involvement). Other comments: controls were sham, negative implantation (Ta pellets used), and positive implantation (Ni pellets used), with 10–20 mice per group, that were observed at 1, 3, 6, 12 ($n = 10$ per group), or 24 mo ($n = 20$ per group). Similar to sham controls, no Ta-implanted mice developed tumours (incidence was thus the same). All Ni-implanted mice developed rhabdomyosarcomas starting 3 mo post-implantation. Pellets were implanted in quadriceps; cylindrical pellets (1 mm in diameter × 2 mm in length). Tumours (rhabdomyosarcomas at implantation site) were not metastatic, unlike those observed in studies carried out in F344 rats (Kalinich et al., 2005; Schuster et al., 2012).

Table 3.1 (continued)

Study design Species, strain (sex) Age at start Duration Reference	Route Agent tested, purity Vehicle Dose(s) No. of animals at start No. of surviving animals	Tumour incidence	Significance	Comments
Full carcinogenicity Rat, F344 (M) 9 wk Up to ~6 mo post-implantation Kalinich et al. (2005)	Intramuscular implantation WGTA (91.1% W, 6.0% Ni, and 2.9% Co) None Pellet(s): 20 Ta (negative control), 4 WGTA + 16 Ta (lower dose), 20 WGTA (higher dose), 20 Ni (positive control) 1× 46, 46, 46, 36 46 at 52 wk [read from Fig. 1], 0 at 38 wk [read from Fig. 1], 0 at 27 wk [read from Fig. 1], 0 at 30 wk [read from Fig. 1]	*Implantation site:* rhabdomyosarcoma 0/46, 46/46*, 46/46*, 36/36*	*[$P < 0.0001$, Fisher exact test]; versus negative control	Principal strengths: well-conducted study, adequate number of rats per group, appropriate statistical analysis, except for tumour incidence (NR). Principal limitations: lack of a group implanted with W only, lack of statistical analysis for tumour incidence. Other comments: intramuscular implantations of pellets on the gastrocnemius muscle of each leg; cylindrical pellets (1 mm in diameter × 2 mm in length). Study duration originally for 24 mo; however, because of the rapid tumour development, no WGTA- or Ni-implanted rat survived much past 6 mo post-implantation. Purity: Ni, 99.995% and Ta, 99.95% Ta. Since rats did not survive for more than 6 mo, the surveillance data included rats designated to be killed at 12, 18, and 24 mo who died earlier. Rapid tumour formation at the implantation site in 100% of the rats, with lung metastasis. The rate of tumour formation correlated with pellet number. Tumours developed rapidly in WGTA-implanted rats as well as in Ni-implanted group (positive control). Palpable tumours were apparent as early as 14 wk post-implantation in some rats at the WGTA higher dose; the tumours were aggressive and fast growing (with metastasis in the lung), necessitating killing of the rats upon becoming moribund several weeks later. Histopathological and immunohistochemical data (use of anti-desmin polyclonal antibody) supported a diagnosis of a pleomorphic rhabdomyosarcoma.

Table 3.1 (continued)

Study design Species, strain (sex) Age at start Duration Reference	Route Agent tested, purity Vehicle Dose(s) No. of animals at start No. of surviving animals	Tumour incidence	Significance	Comments
Full carcinogenicity Rat, F344 (M) 8 wk Up to 24 mo Schuster et al. (2012)	Intramuscular implantation WGTA (91.1 wt% W, 6.0 wt% Ni, and 2.9 wt% Co) None Pellet(s): 20 Ta (negative control), 8 WGTA + 12 Ta (for up to 6 mo), 8 WGTA + 12 Ta (for up to 12 mo) 1× 50, 15, 15 NR	*Implantation site:* rhabdomyosarcoma 0/50, 10/15*, 15/15*	*[$P < 0.0001$, Fisher exact test]	Principal strengths: adequate duration of study, the control groups were adequate (Ta-implanted and untreated controls), adequate number of negative control rats, well-defined adverse effects (tumours and metastasis), appropriate data analysis, except for tumour incidence (NR). Principal limitations: lack of statistical analysis for tumour incidence, small number of rats in the WGTA-implanted groups, no information on number of surviving rats, and the inflammatory components were not addressed properly (e.g. no investigation of myofibroblasts involvement). Other comments: pellets were inserted into the hind legs; cylindrical pellets (1 mm in diameter × 2 mm in length). Mean survival time of the WGTA-treated rats, 36 ± 5.5 wk. Between 6 and 12 mo, 15/15 (100%) of the WGTA-treated rats developed aggressive tumours at the site of implantation and were killed; in 5/15 rats (33%), tumours were found in both legs; thus not all pellets resulted in tumours. 50% of the rhabdomyosarcoma-bearing rats developed metastasis to several organs, mainly the lungs. No rhabdomyosarcomas observed in W-treated and untreated control groups.

Co, cobalt; M, male; mo, month; Ni, nickel; NR, not reported; sham, surgical-sham; Ta, tantalum; W, tungsten; WGTA, weapons-grade tungsten (with nickel and cobalt) alloy; wk, week, wt, weight.

nickel; n = 36), and followed for up to 52 weeks (Kalinich et al., 2005). Because of rapid tumour development, the observation times for rats implanted with WGTA or nickel were only 1, 3, and 6 months. All rats in these groups were killed in a moribund condition before 38 weeks, whereas all rats implanted with tantalum were still alive at 52 weeks. Mean survival for the group implanted with WGTA at the higher dose was significantly lower (21.8 ± 2.1 weeks) than that for the groups implanted with WGTA at the lower dose (27.0 ± 4.6 weeks) or with nickel (25.4 ± 2.1 weeks). Complete necropsies and analyses of histopathology and immunohistochemistry (using an anti-desmin polyclonal rabbit antibody that indicates muscle origin) were performed.

At approximately 16–20 weeks post-implantation, tumours were observed at implantation sites in rats implanted with WGTA or nickel pellets, with palpable tumours detected as early as 14 weeks post-implantation in some rats in the group implanted with WGTA at the higher dose. The tumours were aggressive and fast-growing, necessitating killing of the rats several weeks later. Histopathological examination and immunohistochemical staining identified neoplastic cells that were strongly positive for desmin, suggesting a skeletal muscle origin. At 6 months, all rats implanted with WGTA at the lower (46/46 [$P < 0.0001$, Fisher exact test]) and higher dose (46/46 [$P < 0.0001$, Fisher exact test]) showed rhabdomyosarcoma at the implantation site, whereas none of the 46 tantalum-implanted controls developed tumours. All rats implanted with nickel also developed rhabdomyosarcoma (36/36), although not as rapidly as with WGTA. Tumours metastasized to the lung in WGTA-implanted rats [although the incidence of rats with metastases was not reported], whereas none of the nickel-implanted rats showed signs of metastases. [The Working Group noted this was a well-conducted study, with an adequate number of mice per group. However, there was no group implanted with tungsten only, statistical analysis for tumour incidence was not provided, and the role of inflammatory components was not addressed properly (e.g. there was no investigation of the involvement of myofibroblasts, among other factors).]

Groups of 15 or 50 male Fischer 344 rats (age, 8 weeks) were implanted with 20 pellets (1 mm diameter × 2 mm length; pellets were implanted in a circular pattern and placed approximately 1.5 mm apart), split between each hind leg, of WGTA (91.1% tungsten, 6.0% nickel, and 2.9% cobalt; 4 WGTA pellets and 6 tantalum pellets per leg) or tungsten (4 tungsten pellets and 6 tantalum pellets per leg in the group at the lower dose; 10 tungsten pellets per leg in the group at the higher dose; purity, 100%), and followed for up to 12 months (Schuster et al., 2012). Groups of 15 rats were killed at 3, 6, and 12 months for each implantation group. In addition, four groups of rats were observed for up to 24 months: 50 untreated (controls), 50 implanted with tantalum (negative controls), and 50 implanted with tungsten at the lower or higher dose. Mean survival for the WGTA-implanted group was 36 ± 5.5 weeks, which was comparable to that observed for the group implanted with WGTA at the lower dose in the study by Kalinich et al. (2005). Complete necropsies and histopathological evaluations were performed.

Histopathological examination of all grossly visible tumours was performed and showed that rats implanted with WGTA developed rhabdomyosarcomas at the site of implantation at 6 months (10/15 [$P < 0.0001$, Fisher exact test]) and 12 months (15/15 [$P < 0.0001$, Fisher exact test]) post-implantation, whereas none of the 50 tantalum-implanted negative controls or 50 untreated controls developed tumours after 24 months. Half of the rhabdomyosarcoma-bearing rats had metastases to multiple organs, including the lung, liver, prostate, and lymph nodes. In the group implanted with tungsten at the higher dose, 3/14 rats developed sebaceous adenomas

that surrounded the implanted pellets; these did not progress further over a 22-month period. None of the rats implanted with tungsten at the lower or higher dose developed rhabdomyosarcoma (0/50) (Schuster et al., 2012). [The Working Group noted this was a well-conducted study with adequate duration and control groups; however, only the mean survival time of rats exposed to WGTA was reported. Survival rates at the end of the experiment for controls and exposed rats, and the statistical analysis for tumour incidence, were not reported, the numbers of rats in WGTA-implanted groups were low, and the role of inflammatory components was not addressed properly (e.g. there was no investigation of the involvement of myofibroblasts, among other factors).]

In a study reported in a doctoral dissertation, Shinn (2012) investigated whether positron emission tomography-computed tomography (PET-CT) imaging offers greater sensitivity for the identification of metabolic changes (including inflammation and cell proliferation rates) and primary-stage tumours in muscle tissue surrounding embedded fragments of WGTA when compared with X-rays. Two groups of 17 male Fischer 344 rats (age, 8 weeks) [2 rats per group serving as back-up replacements] were implanted with WGTA (91.1% tungsten, 6% nickel, and 2.9% cobalt) or tantalum (purity, 99.95%; negative controls) pellets (2 pellets/rat, cylinders of 1 mm diameter × 2 mm length, spaced approximately 1.5 mm apart on the lateral side of the right hind leg), and followed for up to 16 weeks (Shinn, 2012). A third group of 2 rats served as sham controls. A series of 1–5 X-rays and ^{18}F-fluoro-2-deoxy-D-glucose PET-CT scans were performed on each rat over 16 weeks (weeks 1, 7, 10, 13, and 16 post-surgery). At scheduled intervals and at 16 weeks post-implantation, the rats were killed. Histopathological examination of tissue around the implants and immunohistochemical staining for desmin and MyoD1 (two biomarkers of myogenic origin, used for the diagnosis of rhabdomyosarcoma) were performed at each time point, as well as measurement of metal concentrations in the urine. The locations of the metal pellets and increased changes in ^{18}F-fluoro-2-deoxy-D-glucose uptake around the pellets were captured on PET-CT images over the 16 weeks. Significant differences in uptake were observed between WGTA-implanted rats and negative controls, with a sensitivity of 86% and specificity of 100%.

WGTA-implanted rats had no visible or palpable tumours at 16 weeks post-implantation; however, they all had histological findings of an invasive disease process: typical skeletal muscle fibres abnormalities, and positive staining for desmin overexpression at 13 weeks post-implantation and for MyoD1 at 7 weeks post-implantation. At 16 weeks, all 15 rats implanted with WGTA developed malignant invasion of fibres of the skeletal muscle, whereas none was reported in the tantalum-implanted negative controls. [The Working Group noted the short duration of observation, the small number of rats per group, and limited reporting and interpretation of the data (e.g. the cellular changes reported by the author were consistent with those observed in malignant tumours and the lesions were not labelled as tumours by the author). Therefore, the Working Group judged the study inadequate for the evaluation of the carcinogenicity of WGTA in experimental animals.]

3.3 Evidence synthesis for cancer in experimental animals

The carcinogenicity of WGTA has been assessed in one study in male mice treated by intramuscular implantation (Emond et al., 2015a) and in two studies in male rats treated by intramuscular implantation (Kalinich et al., 2005; Schuster et al., 2012).

In one study in male B6C3F$_1$ mice exposed to WGTA by intramuscular implantation, there

was a significant increase in the incidence of rhabdomyosarcoma at the implantation site at 6, 12, and 24 months post-implantation when compared with tantalum-implanted or surgical-sham controls (Emond et al., 2015a).

In one well-conducted study in male Fischer 344 rats exposed to WGTA by intramuscular implantation, WGTA at the lower and higher doses caused a significant increase in the incidence of rhabdomyosarcoma at implantation sites when compared with negative controls (Kalinich et al., 2005). In another study in male Fischer 344 rats exposed to WGTA by intramuscular implantation, WGTA caused a significant increase in the incidence of rhabdomyosarcoma at the implantation site at 6 and 12 months post-implantation when compared with negative controls (Schuster et al., 2012).

One study in male Fischer 344 rats exposed to WGTA by intramuscular implantation was considered inadequate for the evaluation of the carcinogenicity of WGTA in experimental animals (Shinn, 2012).

4. Mechanistic Evidence

Studies evaluating absorption, distribution, metabolism, and excretion, and mechanistic evidence for WGTA were performed using either WGTA or simulated WGTA (simulated forms of WGTAs are typically prepared as mixtures of metal microparticles in the same weight ratios as the parent WGTAs). Neither the alloy pellets nor the metal particles had any surface treatment or coating. The pellets were made with tungsten microparticles sintered with nickel and cobalt. Sintering was not reported in the simulated preparations. [The Working Group noted that the effects of sintering with regards to ion release are not known.] WGTAs are named according to the chemical symbols for the component metal elements followed by the percentage of each metal by weight; for example, WNiCo (97–2–1) for a WGTA containing (by weight) 97% tungsten, 2% nickel, and 1% cobalt. Simulated WGTAs are named using an "s" prefix followed by the chemical symbols for the metals and the percentages (by weight) of the metals in the mixture, separated by forward slashes; for example, sW/Ni/Co (92/5/3).

4.1 Absorption, distribution, metabolism, and excretion

4.1.1 Humans

Relevant human exposure to WGTA can result through embedded shrapnel in the body, and/or inhalation of aerosolized particles generated at high temperatures, such as when WGTA hits hard surfaces.

(a) Exposed humans

Only one study has evaluated the exposure of humans to WGTA (Gaitens et al., 2017). This cross-sectional study reported measurements of concentrations of 14 metals in the urine as part of a large case series of United States military veterans with embedded metal fragments resulting from traumatic injury (see Section 1.4.2(b)). [The Working Group noted that none of the veterans had known exposure to the specific tungsten alloy and therefore excluded the study from the evaluation of WGTA.]

(b) Human cells in vitro

No data were available to the Working Group.

4.1.2 Experimental systems

(a) Non-human mammals in vivo

[The Working Group noted that the available data on the absorption, distribution, metabolism, and excretion of WGTAs were limited to absorption (after intramuscular implantation), distribution, and excretion in rodent models.

No data on absorption, distribution, metabolism, and excretion after exposure via the skin or respiratory tract, or on the metabolism of WGTAs after exposure by any route, were available to the Working Group.]

Intramuscular implantation of WGTA pellets consisting of WNiCo (91–6–3) has been used to study metal distribution in serum of male Fischer 344 rats (Kalinich et al., 2008) and multiple organs/tissues of male B6C3F$_1$ mice and male Fischer 344 rats (Emond et al., 2015a; Vergara et al., 2016), and excretion in the urine of male Fischer 344 rats (Kalinich et al., 2008; Schuster et al., 2012; Shinn, 2012) and male B6C3F$_1$ mice (Emond et al., 2015a). [No data on absorption, distribution, metabolism, and excretion in female rodents were available to the Working Group.] Absorption, distribution, metabolism, and excretion of the individual components – tungsten (ICRP, 1981), nickel (WHO, 2000), and cobalt (see the first monograph in the present volume) – have been summarized elsewhere, and are only discussed here in comparison with the same metal in a WGTA.

In rodents with WNiCo (91–6–3) pellets implanted in the muscle, tungsten, nickel, and cobalt were absorbed and distributed systemically (in serum and organs or tissues) and excreted in the urine. [No data on excretion via other routes, such as in the faeces or milk, were available to the Working Group.] High concentrations of these metals were reported in the kidney, spleen, and liver compared with other tissues. Concentrations of tungsten in tissues (kidney, liver, spleen, testes, muscle, and femur, but not brain) and in the urine increased over time until 6–12 months after implantation (Emond et al., 2015a; Vergara et al., 2016). The concentration of tungsten in kidney 6 months post-implantation (at the higher dose) was increased by 7-fold compared with 1 month post-implantation (Vergara et al., 2016). In muscle, only tungsten increased in concentration over time until 6 months (at the higher dose), whereas concentrations of cobalt and nickel decreased between 1 and 6 months post-implantation (Vergara et al., 2016). Compared with tungsten, concentrations of cobalt and nickel in tissues were relatively stable over time (at 1, 3, and 6 months), with notable increases in nickel concentrations in the brain (higher dose) and cobalt concentrations in the liver 6 months post-implantation (Vergara et al., 2016). All three metals in the pellets (tungsten, nickel, and cobalt) have been shown to cross the blood–brain and blood–testes barriers; Emond et al. (2015a) demonstrated that tungsten passes the blood–testes barrier, and Vergara et al. (2016) demonstrated that tungsten, nickel, and cobalt cross the blood–brain and blood–testes barriers. Garrick et al. (2003) showed that cobalt metal binds to a divalent metal transporter 1 isoform (–IRE DMT1), which is predominantly expressed in neuronal cells (Garrick et al., 2003). Soluble tungsten can cross the blood–brain barrier and the placenta (McInturf et al., 2008, 2011, both in US EPA, 2015).

Exposure to WNiCo (91–6–3) caused an increase in metal concentrations in the tissues and urine when compared with WNiFe (97–2–1) or (91–7–2) (Schuster et al., 2012; Emond et al., 2015a). [Although WNiFe alloys are not the agent under evaluation, the Working Group noted that they are informative as control compounds for comparison with WGTAs.] This effect cannot be explained by small differences in the proportions of tungsten and nickel in WNiFe and WGTA pellets, because when the percentage of tungsten or nickel in the WGTA pellets was the same or lower than that in the WNiFe pellets, the concentrations of tungsten and nickel in tissue and urine samples were higher by several fold in groups exposed to WGTA than in groups exposed to WNiFe. It should be noted that the pellets are not homogeneous mixtures of three metals but are composed of tungsten microparticles embedded in a matrix with nickel, cobalt, or iron, and some tungsten (Schuster et al., 2012). [The Working Group noted that tungsten microparticle sizes

were not reported, and that particle sizes could not be estimated from the transmission electron microscopic images because particles were sectioned at various planes and angles.] Higher fractions of nickel and cobalt or iron are present in the matrix than in the whole pellets. After implantation, erosion occurred mostly in the matrix, and WGTA pellets were more deeply eroded than those made of WNiFe. Furthermore, a layer of metal oxide was observed on the surface of WNiFe pellets, but not on the surface of WGTA pellets, and may have functioned as a protective layer against further erosion (and metal release from the WNiFe pellets) (Schuster et al., 2012).

$B6C3F_1$ mice were surgically implanted with pellets composed of one or two metals – tungsten, nickel, and/or cobalt – and tantalum as an inert metal component. Of the cobalt-containing pellets tested (each contained 2.9% cobalt: cobalt with tantalum, tungsten with cobalt and tantalum with 91.1% tungsten, and nickel with cobalt and tantalum with 6% nickel), significant and consistent increases in cobalt concentrations (in the brain, kidney, liver, spleen, femur, testes, serum, and urine; for most of the measured time points: 1, 3, 6, 12, and 24 months) were only measured in the mice exposed to tungsten with cobalt and tantalum (Emond et al., 2015b). [The Working Group noted that the results suggest that the release of cobalt is enhanced by tungsten, but not by nickel.]

(b) Non-human mammalian cells in vitro

No data were available to the Working Group.

4.2 Evidence relevant to key characteristics of carcinogens

This section summarizes the evidence for the key characteristics of carcinogens (Smith et al., 2016), including whether WGTA is genotoxic; induces oxidative stress; induces chronic inflammation; is immunosuppressive; induces epigenetic alterations; causes immortalization; or alters cell proliferation, cell death, or nutrient supply. No data were available for the evaluation of other key characteristics of carcinogens.

4.2.1 Is genotoxic

(a) Humans

(i) Exposed humans

No data were available to the Working Group.

(ii) Human cells in vitro

See Table 4.1.

WGTA pellets and simulated WGTAs increased DNA strand breaks, micronucleus formation, and sister-chromatid exchange in various cultured human cells.

In human primary skeletal muscle cells (HSkMC) in vitro, pellets made of WNiCo (97–2–1) and WNiCo (91–6–3) (207 mm^2 particle surface area/75 cm^2 tissue culture flask), but not WNiFe (97–2–1) or inert tantalum, caused a significant increase in the frequency of DNA strand breaks, as measured by comet assay, after 24 hours of exposure (Harris et al., 2015). [The Working Group noted that the pellets were not cytotoxic at this exposure level based on a Toxilight adenylate kinase assay, but that histological examination had identified regions of dead and dying (apoptotic) cells surrounding the WGTA pellets.]

In an immortalized, non-tumourigenic, human osteosarcoma (HOS) cell line, sW/Ni/Co (92/5/3) caused significant increases in the frequency of DNA strand breaks (at a concentration of ≥ 50 µg/mL, 1-hour exposure, or 5 µg/mL, 24-hour exposure; alkaline elution test), micronucleus formation (at a concentration of ≥ 25 µg/mL, 1-hour exposure, or 5 µg/mL, 24-hour exposure), and sister-chromatid exchange (5 µg/mL dose only) (Miller et al., 2001, 2002). [On the basis of the cytotoxicity reported and other end-points evaluated by the two publications, the Working Group

Table 4.1 Genotoxic effects of weapons-grade tungsten (with nickel and cobalt) alloy or the simulated alloy in human and non-human mammalian cells in vitro

End-point	Tissue, cell type or line	WNiCo or sW/Ni/Co (% of each metal)	Results	Exposure concentration or range, and duration	Comments	Reference
DNA strand breaks (alkaline comet assay)	Primary human skeletal muscle, HSkMC cells	WNiCo (97–2–1) WNiCo (91–6–3), 7 mo after production WNiCo (91–6–3), 39 mo after production WNiCo (91–6–3), 67 mo after production	+ + – +	~207 mm^2 particle surface area per 75 cm^2 tissue culture flask growth area (24-h exposure)	No change in cell viability as measured by Toxilight adenylate kinase assay kit, but histologically there were regions of dead/dying cells surrounding the WNiCo (91–6–3) and WNiCo (97–2–1) pellets. WNiCo (91–6–3) was stored for 7, 39, or 67 mo before testing. [The Working Group noted that storage conditions were not specified.] WNiCo (97–2–1) was not stored. Effect of WNiCo (91–6–3) > WNiCo (97–2–1).	Harris et al. (2015)
DNA strand breaks (rapid alkaline elution test)	Human osteosarcoma, HOS cells (TE85, clone F-5)	sW/Ni/Co (92/5/3)	+	≥ 25 µg/mL (1-h exposure)	50 µg/mL was the lowest exposure concentration at which the response was greater than or equal to that of the positive control (25 µg/mL was also statistically significant at the lowest exposure concentration). Decreased plating efficiency was used for cytotoxicity measurements (> 90% cell viability after 24-h exposure to 50 µg/mL). Reported both particle size and purity. Positive control included.	Miller et al. (2001)
DNA strand breaks (rapid alkaline elution test)	Human osteosarcoma, HOS cells	sW/Ni/Co (92/5/3)	+	5 µg/mL (24-h exposure)	[5 mg/mL was reported in the study, but the Working Group determined that such a high in vitro concentration was most likely a reporting error.]	Miller et al. (2002)

Table 4.1 (continued)

End-point	Tissue, cell type or line	WNiCo or sW/Ni/Co (% of each metal)	Results	Exposure concentration or range, and duration	Comments	Reference
Micronucleus formation (micronucleus assay)	Human osteosarcoma, HOS cells	sW/Ni/Co (92/5/3)	+	≥ 25 µg/mL (1-h exposure)	25 µg/mL was the lowest exposure concentration. Decreased plating efficiency was used for cytotoxicity measurements (> 90% cell viability after 24-h exposure to 50 µg/mL). Reported both particle size and purity. Positive control included.	Miller et al. (2001)
Micronucleus formation (micronucleus assay) Sister-chromatid exchange	Human osteosarcoma, HOS cells	sW/Ni/Co (92/5/3)	+ +	5 µg/mL (24-h exposure) 5 µg/mL (24-h exposure)	Micronuclei measured in binucleate cells. [5 mg/mL was reported in the study, but the Working Group determined that such a high in vitro concentration was most likely a reporting error.]	Miller et al. (2002)
DNA strand breaks (modified alkaline comet assay)	Rat skeletal muscle myoblast, L6-C11 cell line	WNiCo (91–6–3) WNiCo (91–6–3) WNiCo (97–2–1) WNiCo (97–2–1)	+ (with *fpg*) + (without *fpg*) – (with *fpg*) – (without *fpg*) – (ratio of DNA damage levels detected with/without *fpg*) The difference in the DNA damage levels detected with/without *fpg* (*fpg*-sensitive) was not statistically significant.	"Small quantities of particles" with ~207 mm^2 particle surface area in 0.5 mL volume (24-h exposure)	No clear description of concentrations used was reported. Cytotoxicity was indicated histologically by regions of dead/dying cells surrounding the WNiCo (91–6–3) and WNiCo (97–2–1) pellets. No quantitative measurements of cell viability reported. [The Working Group noted that the microscopic images of this study resemble those in Harris et al. (2015), which reported no significant changes in cell viability for WNiCo-exposed samples based on an adenylate kinase assay.]	Harris et al. (2011)

+, positive; –, negative; Co, cobalt; *fpg*, formamidopyrimidine-DNA glycosylase; mo, month; Ni, nickel; sW/Ni/Co, simulated weapons-grade tungsten (with nickel and cobalt) alloy (followed by the percentage of each metal by weight); W, tungsten; WNiCo, weapons-grade tungsten (with nickel and cobalt) alloy (followed by the percentage of each metal by weight).

determined that the reported concentration of 5 mg/mL in Miller et al. (2002) was probably 5 µg/mL.] Median diameters (d_{50}) of particles were 1–4 µm for cobalt, 3–5 µm for nickel, and 1–3 µm for tungsten. [The Working Group noted that exposure to the simulated WGTA caused minimal cytotoxicity at the 50 µg/mL dose. Also, injection of the HOS (TE85, clone F-5) cells into 128 (Miller et al., 2001) and 82 (Miller et al., 2002) athymic nude mice (strain/breed not reported) did not cause any tumour development up to 6 months after injection. However, in a study by Lauvrak et al. (2013), the incidence of tumours after injection of HOS (CRL-1543) cells into NOD/SCID/IL2r gamma^{null} (NSG) mice was 12/12 mice within 10–20 days post-injection.]

[The lack of effect of WNiFe, compared with WGTA, is probably caused by decreased metal release after the formation of a metal oxide layer on the surface of WNiFe (but not WGTA) pellets (Schuster et al., 2012). Miller et al. (2001) pointed out that the induction of DNA strand breaks by simulated WGTA was more than the sum of the induction of DNA strand breaks by the individual metals at concentrations matching those in the simulated WGTA.]

(b) Experimental systems

(i) Non-human mammals in vivo

No data were available to the Working Group.

(ii) Non-human mammalian cells in vitro

See Table 4.1.

In a rat skeletal-muscle myoblast cell line (L6.C11), there was a significant increase in the incidence of DNA strand breaks (as measured by modified comet assay) after exposure to WNiCo (91–6–3), but not WNiCo (97–2–1) or WNiFe (97–2–1), for 24 hours (Harris et al., 2011) [see also Section 4.2.2(b)(ii)]. Cytotoxicity was indicated histologically by regions of dead and dying cells surrounding the WNiCo (91–6–3) and WNiCo (97–2–1) pellets. [The Working Group noted that the concentrations used were not clearly described. In addition, cell viability measurements were not reported, and microscopic images resembled those reported in Harris et al. (2015).]

[The Working Group noted that muscle implantation of WNiCo (92–6–3) caused rhabdomyosarcoma in Fischer 344 rats (Kalinich et al., 2005; Schuster et al., 2012) and B6C3F$_1$ mice (Emond et al., 2015a). No bioassay evidence for WNiCo (97–2–1) was available to the Working Group. The Working Group also noted the possibility of species differences related to exposure to WNiCo (97–2–1), which gave positive results for genotoxicity in human cells.]

4.2.2 Induces oxidative stress

(a) Humans

No data were available to the Working Group.

(b) Experimental systems

(i) Non-human mammals in vivo

Oxidative stress was suggested by changes in urinary metabolite concentrations, as measured by ^{1}H nuclear magnetic resonance spectroscopic profiling, in male Sprague-Dawley rats injected intraperitoneally with 0.5 mL sW/Ni/Co (91/5/4) at one of two doses (Tyagi et al., 2014). The lower doses were reported to be one tenth to one fifth of the median lethal dose (LD_{50}; per kg bw), while the higher doses were two to four fifths of the LD_{50}. [The Working Group noted that it was not clear if the LD_{50} values were for individual metals or for the combined simulated WGTA mixture, and LD_{50} values were not reported.] Urinary concentrations of *N*-methylnicotinamide were increased significantly 8 hours after injection of the higher dose and decreased significantly 72 hours after injection of the lower dose. Creatinine and choline levels were increased significantly 8–120 hours after injection of the higher or lower dose. Not all changes were significant at all time points, and the measured

metabolites could be linked to different metabolic pathways (including glutathione), or enzymes related to oxidative stress (Tyagi et al., 2014). [The Working Group noted other possible causes of the observed increases, which were not explored and therefore cannot be ruled out.]

(ii) Non-human mammalian cells in vitro

Concentrations of reactive oxygen species (ROS) were increased significantly in a rat skeletal muscle myoblast cell line (L6.C11) as early as 1 hour after exposure to WNiCo (91–6–3) and WNiCo (97–2–1), but not WNiFe (97–2–1) (Harris et al., 2011). The increase in ROS was greatest for WNiCo (91–6–3), followed by WNiCo (97–2–1), and then WNiFe (97–2–1), which was also the same ranking for cytotoxicity. After exposure to WNiCo (91–6–3) for 24 hours, there was a significant increase in the frequency of DNA strand breaks, as measured by modified comet assay with DNA-formamidopyrimidine glycosylase enzymatic cleavage. However, the difference in incidence measured with or without DNA-formamidopyrimidine glycosylase enzymatic cleavage was not statistically significant. In line with the observed changes in ROS, exposure to WNiCo (97–2–1) and WNiFe (97–2–1) with DNA-formamidopyrimidine glycosylase enzymatic cleavage did not increase DNA damage (Harris et al., 2011) (see Table 4.1).

In primary pulmonary macrophages collected from BAL fluid obtained from male Sprague-Dawley rats, exposure to 12.5–200 µg/mL of sW/Ni/Co (92/5/3) caused a significant increase in intracellular ROS and reactive nitrogen species (measured together and including hydrogen peroxide, peroxyl radical, nitric oxide, and peroxynitrite anion) 1 hour after exposure compared with controls (Roedel et al., 2012). Exposure to concentrations of 100 µg/mL or greater caused a significant decrease in cell viability. Median particle sizes were 1–5 µm for tungsten, 3–7 µm for nickel, and 1.6 µm for cobalt.

4.2.3 Evidence relevant to other key characteristics of carcinogens

(a) Induces chronic inflammation

(i) Exposed humans

A case report of occupational asthma (an indicator of a chronic inflammatory response) in a French hard-metal industry worker evaluated the occupational history and the effects of exposure to tungsten on the lower respiratory system (via BAL). There was co-exposure to multiple metals, including tungsten carbide, nickel, cobalt, and chromium. Mechanistic assessments (allergic reactions) were carried out for nickel and cobalt, but not for tungsten (De Hauteclocque et al., 2002). [The Working Group noted that the assessment was not specific to tungsten alloys and excluded the study from the evaluation of WGTA (see Table S1.4; Annex 1, Supplementary material for Section 1, Exposure Characterization, web only, available from: https://publications.iarc.fr/618).]

(ii) Human cells in vitro

In one study of human hepatoma (HepG2) cells in vitro, exposure to sW/Ni/Co (92/5/3) (5–50 µg/mL) caused a significant increase in the expression of 6/13 stress gene promoters/response elements after 48 hours, as measured by CAT-Tox (L) (chloramphenicol acetyl transferase-toxicity (L)iver) reporter assay (Miller et al., 2004). Two of the genes were related to immune function: NFκBRE (serving as a binding site for the transcription factor NFκB, also known as NFKB1) and CRE (serving as a binding site for CREB protein, which is activated by pro-inflammatory signals and various transcription factors, and also known as Cre recombinase) (Wen et al., 2010). [The Working Group noted that the cell viability was greater than 85% at ~5 µM.]

(iii) Experimental systems

While no studies directly evaluating chronic inflammation were available to the Working Group, acute changes in biomarkers of inflammation and immune activation were reported in vivo (Roedel et al., 2012). Pulmonary inflammation was shown histologically by increased numbers of inflammatory cells (including neutrophils) in the lung tissues of male Sprague-Dawley rats 24 hours after intratracheal instillation of sW/Ni/Co (92/5/3) at 20 and 40 mg/kg bw, compared with controls instilled with saline or tungsten alone (Roedel et al., 2012). Acute inflammation was also indicated by significant increases in numbers of neutrophils, and levels of Cinc-1, Cinc-3, Tnfb, Il1b, and albumin proteins in the BAL fluid of treated rats, compared with controls. In addition, quantification of messenger RNA (mRNA) of several genes related to inflammation indicated significant differences in lung tissue and cells from BAL fluid of treated rats compared with controls (Roedel et al., 2012) (see also Section 4.2.4).

Male Fischer 344 rats were chronically exposed to WNiCo (91–6–3) at a lower (4 pellets/rat) or higher (20 pellets/rat) dose administered by intramuscular implantation for 3 months (i.e. those animals that did not die or were not killed early due to incidence of rhabdomyosarcoma). Both treatment groups showed a significant increase in peripheral blood counts for total leukocytes, neutrophils, lymphocytes, and monocytes (but not eosinophils or basophils) compared with controls implanted with tantalum pellets, and a significant increase in spleen weights in the group at the higher dose (Kalinich et al., 2005). In the group at the higher dose, significant increases in neutrophil counts and spleen weights were observed by 1 month compared with controls (Kalinich et al., 2005). In killed rats, counts of total leukocytes, neutrophils, lymphocytes, monocytes, and eosinophils, and spleen weights were increased significantly in the group at the higher dose, while neutrophil counts were increased significantly in the group at the lower dose. However, in one study by Shinn (2012), no significant changes in haematology parameters, i.e. total leukocytes or any specific immune or inflammatory cells (lymphocytes, monocytes, or granulocytes), were observed in rats treated with the same WGTA (or tantalum) pellets up to 16 weeks post-implantation.

(b) Is immunosuppressive

Experimental systems

In Fischer 344 male rats, chronic exposure to WNiCo (91–6–3) (20 pellets/rat) administered by intramuscular implantation for up to 5 months caused a significant decrease in thymus-to-body-weight ratio (Kalinich et al., 2005).

In primary pulmonary macrophages collected from BAL fluid of untreated male Sprague-Dawley rats, exposure to sW/Ni/Co (92/5/3) (25–200 µg/mL) caused a significant decrease in phagocytosis of (non-opsonized) zymosan particles after 1 hour (Roedel et al., 2012). Exposure concentrations of ≥ 100 µg/mL caused a significant decrease in cell viability. Phagocytosis was measured using a CytoSelect 96-well phagocytosis assay and was also observed by microscopy for a subset of cells.

(c) Induces epigenetic alterations

Epigenetic changes induced by exposure to sW/Ni/Co (91/6/3) were studied in four cell types in vitro (two of human and two of mouse origin): human embryonic kidney (HEK-293) and neuroepithelioma (SK-N-MC) cell lines, and mouse hippocampal primary neuronal cell cultures and a myoblast (C2C12) cell line (Verma et al., 2011). Exposure times were 1 week for the mouse primary neuronal cell cultures and 1 day for the other cell types. sW/Ni/Co (91/6/3) was cytotoxic at concentrations greater than 50 µg/mL. Exposure to simulated WGTA (183.9 µg/mL) caused a significant decrease in

the phosphorylation of serine 10 on histone 3 in primary neuronal cell cultures and C2C12 cells, and significant decreases were measured in all four cell types after exposure to cobalt alone (58.9 µg/mL). Exposure to simulated WGTA and cobalt alone also caused a significant decrease in the acetylation of histone 3 in C2C12 cells and in all cell types except primary neuronal cell cultures, respectively. Trimethylation of lysine 4 on histone 3 was not affected by exposure to simulated WGTA or cobalt. Additionally, exposure to nickel did not induce any of these epigenetic changes in the four cell types studied. Further investigation of histone modifications induced by exposure to simulated WGTA and cobalt in C2C12 cells showed that an intracellular calcium chelator (but not an extracellular calcium chelator or calcium channel blocker) reversed simulated WGTA- and cobalt-induced hypophosphorylation of serine 10 on histone 3, suggesting that this epigenetic effect may be due to increased concentrations of intracellular calcium or changes in intracellular calcium dynamics (Verma et al., 2011).

Histone modification was further supported by the study of Harris et al. (2011), which showed that exposure to WNiCo (91–6–3) caused significant upregulation in mRNA levels of histone methylase, histone acetylase, and histone deacetylase in rat L6-C11 cells but induced an increase in protein levels of histone 2A only. Quantification of mRNA expression revealed a significant increase in histone deacetylase mRNA, but not histone methylase or histone acetylase mRNA, after exposure to WNiCo (97–2–1). Exposure to WNiCo (97–2–1) caused a greater increase in histone 2A protein concentrations than did exposure to WNiCo (91–6–3).

(d) Causes immortalization

In HOS cells cultured in vitro, exposure to sW/Ni/Co (92/5/3) at a non-cytotoxic concentration of 50 µg/mL for 24 hours caused a significant increase in the frequency of neoplastic transformation (with increased anchorage-independent cell growth in soft agar) and invasion (through Matrigel) over a 5-week period in vitro, compared with untreated cells. Untreated HOS cells are not tumourigenic; subcutaneous injection of these cells did not cause any tumours in 128 female athymic nude mice after 6 months. In contrast, HOS cells transformed with sW/Ni/Co (92/5/3) caused adenocarcinoma in 6 out of 12 mice within 4 weeks. Transformation of HOS cells with sW/Ni/Co (92/5/3) caused a significant increase in the expression of K-*ras* oncogene mRNA, and the adenocarcinomas gave positive results for cytokeratin (an epithelial cell marker) and negative for vimentin (a mesenchymal cell marker) (Miller et al., 2001). [The Working Group noted that this suggested that there was no epithelial–mesenchymal transition.] Exposure of HOS cells to sW/Ni/Co (92/5/3) at a non-cytotoxic concentration of 10 µg/mL for 24 hours also caused a significant increase in the frequency of neoplastic transformation (with increased anchorage-independent cell growth in soft agar) in vitro compared with untreated cells. Injection of the untreated cells did not cause any tumours in 82 athymic nude mice after 6 months. In contrast, sW/Ni/Co (92/5/3)-transformed cells caused adenocarcinoma in 8 out of 20 mice within 4 weeks (Miller et al., 2002). [The Working Group noted that the metal that contributed to the transformation of HOS cells in vitro was probably nickel, because nickel (but not tungsten or cobalt) at a concentration equivalent to that in sW/Ni/Co (92/5/3) induced a small but significant increase in transformation frequency in vitro in the study by Miller et al. (2001). Nickel also increased the transformation frequency in Miller et al. (2002), but nickel-transformed cells did not consistently cause tumours in the athymic nude mice, with tumour incidence reported to be 0/12 in Miller et al. (2001) and 6/20 in Miller et al. (2002).]

4.2.4 Multiple characteristics identified via microarray or omics

(a) Humans

(i) Exposed humans

No data were available to the Working Group.

(ii) Human cells in vitro

See Table 4.2.

Exposure to WNiCo (91–6–3) (stored for 7, 39, or 67 months) for 24 hours induced changes in many pathways related to key characteristics in human primary HSkMC cells cultured in vitro. [The Working Group noted that freshly made WNiCo (91–6–3) was not tested.] On the basis of annotation enrichment analysis, there was increased expression of mRNA transcripts relevant to immune/pro-inflammatory responses and cytokine–cytokine receptor interactions, the oxidative stress response (including NRF2), components of the glutathione system, antioxidant enzymes, the response to hypoxia, increased glycolysis and angiogenesis, and decreased cell death (increased expression of mRNA transcripts associated with negative regulation of apoptosis including anti-apoptosis, wound healing, and regulation of cell proliferation). Decreased expression of mRNA transcripts for immunoglobulins, muscle-specific proteins and contractile fibres, the actin cytoskeleton, and cell differentiation-associated genes indicated that immune function and muscle tissue differentiation were decreased (Harris et al., 2015). Exposure of HSkMC cells to WNiCo (97–2–1) in vitro caused transcriptional changes that were similar to those caused by exposure to WNiCo (91–6–3), albeit in fewer genes. [The Working Group noted that decreased differentiation is critical to carcinogenesis because, when they do not terminally differentiate, cells may maintain the ability to multiply and/or proliferate, which increases their likelihood of transformation.] Caspase-3 activity was not altered in HSkMC cells exposed to WNiCo (97–2–1), WNiCo (91–6–3), or WNiFe (97–2–1) in vitro for 24 hours (Harris et al., 2015). [The Working Group noted that this is consistent with gene expression, indicating anti-apoptotic effects. Moreover, the Working Group noted possible species differences, because human cells were less sensitive to the effects of WNiCo (91–6–3) than rat L6.C11 cells in vitro (based on measurement of caspase-3 activity and the number of genes with altered expression), to which the authors refer in their previous study (Harris et al., 2011) (see also Section 4.2.4(b)(ii) and Table 4.3).]

(b) Experimental systems

(i) Non-human mammals in vivo

See Table 4.3.

In addition to the evaluation of immune/pro-inflammatory responses by assessment of phagocytosis, concentrations of cytokines in BAL fluid, and lung histology (see also Section 4.2.4), cells collected from BAL fluid from male Sprague-Dawley rats exposed to sW/Ni/Co (92/5/3) (20 mg/kg bw) by intratracheal instillation were assessed by Rat Stress and Toxicity PathwayFinder RT^2 Profiler PCR Array (expression of 84 genes was assessed). Significant differences in mRNA transcript expression compared with cells from control rats exposed to saline were related to signalling pathways involved in apoptosis (increased NFkbia and decreased Casp1 expression), growth arrest and senescence (increased Cdkn1a and Ddit3), cell proliferation (decreased E2f1), and inflammation (increased Il6, Mip-1a, Mip-1b, Il1b, Tnfb, and Nos2/iNOS, and GM-CSF, and decreased Il18) (Roedel et al., 2012). In lung tissue collected from rats exposed to sW/Ni/Co (92/5/3) via intratracheal instillation (i.e. they did not undergo the BAL procedure), significant differences in mRNA transcript expression were only observed for two genes, with increased expression of Il6 and decreased expression of cytochrome P450, family 2, subfamily A, polypeptide 3 (CYP2A3)

Table 4.2 Microarray and omics results for multiple key characteristics after exposure to weapons-grade tungsten (with nickel and cobalt) alloy or the simulated alloy in human cells in vitro

End-point	Platform	Results	Relevant KCs[a]	Tissue, cell type or line	Test article, exposure concentration or range, and duration	Comments	Reference
Expression of 13 stress gene promoter/ response elements	CAT-Tox (L) reporter assay (ELISA)	Increased induction of gene promoters related to metal sequestration (hMTIIA), oxidative stress and immune function (FOS and NFκBRE), DNA/protein damage (P53RE and HSP70), and the binding site for CREB (CRE)	KCs 2,3, 5, and 6	Human hepatoma, 13 HepG2-derived cell lines transfected with gene promoter-CAT fusion constructs (CAT-Tox (L) reporters)	sW/Ni/Co (92–5–3), 5–50 μg/mL, 48-h exposure	Cell viability was > 85% at ~5 μM. CREB is involved in the differentiation of T lymphocytes, among other functions.	Miller et al. (2004)

Table 4.2 (continued)

End-point	Platform	Results	Relevant KCs[a]	Tissue, cell type or line	Test article, exposure concentration or range, and duration	Comments	Reference
Transcriptomics	Microarray slides (Agilent human gene expression microarray kit 4×44K; Design ID 026652)	WNiCo (91–6–3) induced decreased expression of mRNA transcripts encoding muscle-specific proteins and contractile fibres, components of the actin cytoskeleton, cell differentiation-associated proteins, and immunoglobulins WNiCo (91–6–3) and WNiCo (97–2–1) induced increased expression of mRNA transcripts encoding components of the glycolic and pentose phosphate pathways, response to hypoxia, immune response, cytokine–cytokine receptor interactions, anti-apoptotic pathways, wound healing, and regulation of cell proliferation WNiCo (91–6–3) induced increased expression of mRNA transcripts encoding components of the oxidative stress response (including NRF2), glutathione metabolic system, antioxidant enzymes (SOD1, SOD2, PRDX1, SRXN1, and NQO1), pro-inflammatory response, and angiogenesis (VEGFA)	KCs 5, 6, 7, and 10	Primary human skeletal muscle, HSkMC cells	WNiCo (91–6–3), WNiCo (97–2–1), ~207 mm^2 particle surface area per 75 cm^2 tissue culture flask growth area, 24-h exposure	The effects of WNiCo (91–6–3) and WNiCo (97–2–1) were similar qualitatively, but exposure to WNiCo (97–2–1) altered the expression of fewer genes. WNiCo (91–6–3) was stored for 7, 39, or 67 mo before testing. [The Working Group noted that storage conditions were not provided.] Longer storage time caused a decrease in the number of genes with altered expression. WNiCo (97–2–1) was not stored.	Harris et al. (2015)

CAT-Tox (L), chloramphenicol acetyl transferase-toxicity (L)iver; Co, cobalt; CREB (CRE), cAMP response element; ELISA, enzyme-linked immunosorbent assay; FOS, Fos proto-oncogene, AP-1 transcription factor subunit; hMTIIA, human metallothioneinIIA; KC, key characteristic; mo, month; mRNA, messenger RNA; NFκBRE, nuclear factor kappa (B site) response element; Ni, nickel; p53RE, 53 kDa protein tumour suppressor response element; PRDX1, peroxiredoxin; SOD, superoxide dismutase; SRXN1, sulfiredoxin; sW/Ni/Co, simulated weapons-grade tungsten (with nickel and cobalt) alloy (followed by the percentage of each metal by weight); VEGFA, vascular endothelial growth factor; W, tungsten; WNiCo, weapons-grade tungsten (with nickel and cobalt) alloy (followed by the percentage of each metal by weight).

[a] Key characteristic 2, is genotoxic; key characteristic 3, alters DNA repair or causes genomic instability; key characteristic 5, induces oxidative stress; key characteristic 6, induces chronic inflammation; key characteristic 7, is immunosuppressive; key characteristic 10, alters cell proliferation, cell death, or nutrient supply.

Table 4.3 Microarray and omics results for multiple key characteristics after exposure to weapons-grade tungsten (with nickel and cobalt) alloy or the simulated alloy in non-human mammals in vivo and non-human mammalian cells in vitro

End-point	Platform	Results	Relevant KCs[a]	Tissue, cell type or line	Test article, exposure concentration or range, and duration	Comments	Reference
Gene expression	RT-PCR array (Rat Stress and Toxicity PathwayFinder RT^2 Profiler PCR Array (84 genes), QIAGEN)	BAL cells with altered expression of mRNAs encoding proteins related to apoptosis signalling (↑ Nfkbia and ↓ Casp1), growth arrest and senescence (↑ Cdkn1a and Ddit3), heat shock (↑ Hspa1a), inflammation (↑ Il6, Mip-1a, Mip-1b, GM-CSF, Il1b, Tnfb, and Nos2/iNOS, and ↓ Il18), and cell proliferation (↓ E2f1) Lung tissue with 2/84 genes assayed with differential expression (↑ Il6 and ↓ CYP2A3)	KCs 5, 6, and 10	Primary BAL cells and lung tissue	sW/Ni/Co (92–5–3), 20 mg/kg bw, intratracheal instillation of male SD rats, 24-h exposure		Roedel et al. (2012)
Metabolomics	^{1}H NMR spectroscopy	↓ NMN (lower dose at 8 and 24 h), ↑ NMN (higher dose at 8, 24, and 72 h), ↑ choline (lower dose at 8 h, higher dose at 24, 72, and 120 h), ↑ creatinine (lower dose at 8 and 24 h, higher dose at 24 and 72 h), and ↓ gut flora metabolite (hippurate) (lower dose at 72 h, higher dose at 24, 72, and 120 h) Altered metabolic pathways (at 24 h) were TCA cycle; alanine, aspartate, and glutamate (amino acid) metabolism; butanoate metabolism; and glyoxylate and dicarboxylate (carbohydrate) metabolism	KCs 5 and 10	Urine	sW/Ni/Co (91/5/4), 0.5 mL intraperitoneal injection of male SD rats (lower and higher dose), 8, 24, 72, and 120-h exposure	The Working Group noted that NMN changes may be due to oxidative stress in the liver. Lower dose was one tenth of LD_{50} per kg bw. Higher dose was two fifths to four fifths of the LD_{50} per kg bw.	Tyagi et al. (2014)

Table 4.3 (continued)

End-point	Platform	Results	Relevant KCs[a]	Tissue, cell type or line	Test article, exposure concentration or range, and duration	Comments	Reference
Transcriptomics	Microarray (Rat Genome 230 2.0 whole-genome oligonucleotide arrays, Affymetrix, Inc.)	↑ Expression of cell cycle-related genes; ↓ expression of muscle development and differentiation genes Top 3 KEGG pathways altered (adherens junction, p53 signalling pathway, and cell cycle) ↑ Expression of genes common to cancer including sarcoma (CCND1, CDKN2A, MDM2, CDK4, and MAPK3) ↑ Expression of genes on chromosomal cytoband 7q22 including MDM2 (binds/inhibits p53), CDK4 (G1 phase progression), WiF1 (inhibits Wnt signalling), OS9 (amplified in osteosarcoma), SLC35E3, and XRCC6 (DNA repair double-strand breaks)	KCs 3 and 10	Tumours (rhabdomycosarcomas)	Intramuscular WNiCo (91–6–3), 4 pellets per leg + 6 Ta pellets per leg (10 pellets per leg total) per male F344 rat		Schuster et al. (2012)

Table 4.3 (continued)

End-point	Platform	Results	Relevant KCs[a]	Tissue, cell type or line	Test article, exposure concentration or range, and duration	Comments	Reference
Transcriptomics	Microarray slides (prepared from a set of rat AROS V3.0 oligonucleotides (Eurofins MWG Operon, Alabama, USA) by the Functional Genomics Facility at the School of Biosciences, University of Birmingham, UK)	5 functional areas affected WNiCo (9–6–3) altered 4 areas (induced ↓ expression of mRNA transcripts encoding components of muscle structure/function; induced ↑ expression of mRNA transcripts encoding protein components of carbohydrate metabolism/glycolysis, DNA damage/stress response, and apoptosis/cell death) WNiCo (97–2–1) altered 3 areas (induced ↓ expression of mRNA transcripts encoding protein components of muscle structure/function; induced ↑ expression of mRNA transcripts encoding proteins involved in DNA organization/regulation and carbohydrate metabolism/glycolysis)	KCs 2,3, 4, 5, and 10	Rat skeletal muscle myoblasts, L6-C11 cell line	WNiCo (91–6–3) and WNiCo (97–2–1), "Small quantities of particles" with ~207 mm^2 particle surface area in 0.5 mL volume, 24- or 48-h exposure	No clear description of concentrations used was reported. No quantitative measurements of cell viability reported.	Harris et al. (2011)

Table 4.3 (continued)

End-point	Platform	Results	Relevant KCs	Tissue, cell type or line	Test article, exposure concentration or range, and duration	Comments	Reference
Transcriptomics	Microarray (RatRef-12 v1.0 Expression and MouseRef-8 v2.0 Expression BeadChips, Illumina); qRT-PCR for validation of selected genes	↑ FN3K expression, significantly altered compared with control (Ta) exposure in rat L6-C11 cells ↑ Fos expression, but not significantly altered compared with control.	KCs 5 and 10	Rat skeletal muscle myoblasts, L6-C11 cell line Mouse skeletal muscle myoblasts, C2C12 cell line	sW/Ni/Co (91/6/3), 10 µg/mL, 24-h exposure		Bardack et al. (2014)

↓, decreased; ↑, increased; BAL, bronchoalveolar lavage; bw, body weight; Co, cobalt; CYP2A3, cytochrome P450, family 2, subfamily A, polypeptide 3; ^{1}H NMR, ^{1}H nuclear magnetic resonance; KC, key characteristic; KEGG, Kyoto Encyclopaedia of Genes and Genomes; LD_{50}, median lethal dose; mRNA, messenger RNA; Ni, nickel; NMN, *N*-methyl nicotinamide; qRT-PCR, real-time quantitative reverse transcription polymerase chain reaction; RT-PCR, real-time polymerase chain reaction; SD, Sprague-Dawley; sW/Ni/Co, simulated weapons-grade tungsten (with nickel and cobalt) alloy; Ta, tantalum; TCA, tricarboxylic acid; W, tungsten.

[a] Key characteristic 2, is genotoxic; key characteristic 3, alters DNA repair or causes genomic instability; key characteristic 4, induces epigenetic alterations; key characteristic 5, induces oxidative stress; key characteristic 6, induces chronic inflammation; key characteristic 7, is immunosuppressive; key characteristic 10, alters cell proliferation, cell death, or nutrient supply.

(Roedel et al., 2012). Histological assessment of protein expression in lung tissue by immunohistochemical analysis also showed that CYP2A3 protein expression was decreased. [The Working Group noted that differences in CYP2A3 mRNA expression are related to metabolism but are unlikely to be related to oxidative stress.]

Metabolomics analysis of urine samples collected from rats after intraperitoneal injection of sW/Ni/Co (91/5/4) (see Section 4.2.2 for doses) showed alterations in nutrient supply (Tyagi et al., 2014). Significant changes in energy metabolism (including the tricarboxylic acid cycle, amino acid metabolism, and carbohydrate metabolism) were observed in the urinary metabolomics profile 24 hours after exposure.

Schuster et al. (2012) performed microarray analysis to identify altered mRNA transcript expression in rhabdomyosarcomas from male Fischer 344 rats exposed to WNiCo (91–6–3) pellets by intramuscular implantation. Exposure to WNiCo (91–6–3) caused a significant increase in the expression of cell cycle-related genes and decreased expression of genes involved in muscle development and differentiation (see Table 4.3).

(ii) Non-human mammalian cells in vitro

See Table 4.3.

As in the study by Harris et al. (2015) that used human primary HSkMC cells, transcriptomics analysis of rat L6.C11 cells treated with WNiCo (97–2–1) or WNiCo (91–6–3) showed increased carbohydrate metabolism (of enriched functional groups), and increased expression of mRNA transcripts associated with glycolysis and response to hypoxia (Harris et al., 2011). [The Working Group noted that this suggested that WGTA drives cells towards anaerobic glycolysis, also known as the Warburg effect.] Exposure to WNiCo (97–2–1) and WNiCo (91–6–3) also caused a significant decrease in the expression of mRNA transcripts of genes related to cell differentiation, specifically genes involved in muscle structure and function (Harris et al., 2011). [The Working Group noted that exposure to WGTA caused rhabdomyosarcoma in both mice (Emond et al., 2015a) and rats (Kalinich et al., 2005; Schuster et al., 2012) (see Section 3), and that evidence of blocked differentiation of muscle cells was observed in rhabdomyosarcoma in humans (Sirri et al., 2003).] In addition, exposure of rat L6.C11 cells to WNiCo (91–6–3), WNiCo (97–2–1), and WNiFe (97–2–1) caused a significant decrease in (pro-apoptotic) caspase-3 activity after 24 hours (Harris et al., 2011, 2015), but this was not observed in human primary HSkMC cells (Harris et al., 2015). [The Working Group noted possible species differences since human cells were less sensitive to the effects of WNiCo (91–6–3) than rat L6.C11 cells on the basis of caspase-3 activity and the number of genes with altered expression as reported in Harris et al. (2011), to which the authors refer.] Increased glycolysis was suggested by a significant increase in the expression of fructosamine 3 kinase (Fn3k) mRNA transcripts in rat L6.C11 cells treated with sW/Ni/Co (91/6/3) at 10 µg/mL for 24 hours, as assessed by microarray analysis and quantitative real-time polymerase chain reaction validation (Bardack et al., 2014). Fn3k can de-glycate Nrf2 (also known as Nfe2l2), which activates its oncogenic function, although how glycation affects the function of other Fn3k-sensitive proteins (e.g. translation factors, heat shock proteins, and histones) is not clear (Sanghvi et al., 2019). Fos expression, which is relevant to oxidative stress, was also increased in rat L6.C11 cells exposed to sW/Ni/Co (91/6/3) in vitro, but was not significantly different compared with controls exposed to tantalum, which is inert (Bardack et al., 2014).

Adams et al. (2015) treated rat pheochromocytoma (PC-12) cells with sW/Ni/Co (55/33/17), which was composed of a mixture of soluble ionic metal salts (from sodium tungstate, nickel acetate, and cobalt acetate) based on their predominant oxidation states and metal ratios in the leachate of WNiCo (91–6–3) alloy, in cell culture media for 24 hours. Microarray experiments using

Affymetrix GeneChip Rat Genome 230 2.0 chips showed that expression of only a few mRNA transcripts was altered by exposure to sW/Ni/Co (55/33/17) at concentrations of ~3 μg/mL for tungsten, 2 μg/mL for nickel, and 1 μg/mL for cobalt. Pathway enrichment analysis could not be performed because too few genes had altered expression.

4.2.5 Other adverse effects

Although not directly measured, the gut microbiome is a potential target of sW/Ni/Co. Exposure of rats to sW/Ni/Co (91/5/4) by intraperitoneal injection caused significant alterations in gut flora metabolites (decreased hippurate) and butanoate metabolism, as assessed by profiling of urinary metabolites (Tyagi et al., 2014). Butanoate metabolites include short-chain fatty acids and alcohols, which are typically produced by fermentation in the intestine. Both nickel and cobalt have been shown to alter the diversity and composition of the gut microbiome in rats exposed to these metals by gavage (Richardson et al., 2018).

5. Summary of Data Reported

5.1 Exposure characterization

Weapons-grade tungsten (with nickel and cobalt) alloys (WGTAs) typically contain 91–93% tungsten, 3–5% nickel, and 2–4% cobalt. During the 1990s, the search for alternatives to lead and depleted uranium resulted in the investigation and use of these tungsten alloys in kinetic energy penetrators, guided missiles, and other types of armour-piercing munitions.

Inhalation is probably the primary route of exposure for occupationally exposed populations. Occupational exposure to the elements contained in WGTA may occur during the manufacture and production of munitions. In addition, military personnel and civilians can be exposed to metal aerosols generated during the firing of WGTA munitions and on impact with their targets. Individuals with ammunition-related injuries may have retained embedded fragments containing the WGTA, which may lead to long-term exposure to metal ions released from the fragments. There are few studies in the published literature that quantify exposures for these different scenarios.

No regulations were identified to date concerning exposure to WGTAs; however, exposure limits and guidelines for its individual elemental constituents (tungsten, nickel, and cobalt) do exist.

5.2 Cancer in humans

No data were available to the Working Group.

5.3 Cancer in experimental animals

Treatment with WGTA caused an increase in the incidence of malignant neoplasms in two species.

WGTA administered by intramuscular implantation in one study in male B6C3F$_1$ mice caused an increase in the incidence of rhabdomyosarcoma at the implantation site.

In two studies, WGTA administered by intramuscular implantation in male Fischer 344 rats caused an increase in the incidence of rhabdomyosarcoma at the implantation site.

5.4 Mechanistic evidence

Data on absorption, distribution, and excretion were available from studies on intramuscular implantation of WGTA pellets in rodents. Tungsten, nickel, and cobalt in the implanted WGTA were absorbed, distributed systemically (including to the brain and testes), and excreted in the urine. Concentrations of these metals

were higher in the kidney, spleen, and liver than in other tissues. Tungsten concentrations in the tissues and urine increased over the course of 1, 6, and 12 months after implantation, while nickel and cobalt tissue concentrations stabilized over 1 to 6 months, with noticeable increases in cobalt concentrations in the liver and nickel in the brain. Nickel and cobalt were shown to be more readily released from WGTA than was tungsten.

Overall, the mechanistic evidence is suggestive but sparse, based on only a few available studies in experimental systems. There was one study in exposed humans that was uninformative to the evaluation because the exposure was not to WGTA. Evidence was suggestive for the key characteristics "is genotoxic", "induces epigenetic alterations", "induces oxidative stress", "is immunosuppressive", and "alters cell proliferation, cell death, or nutrient supply" in experimental systems.

There is suggestive evidence that WGTA is genotoxic based on induction of DNA damage and micronucleus formation by WGTA and/or simulated WGTA (sW/Ni/Co) in vitro. WNiCo (91–6–3) and WNiCo (97–2–1) at non-cytotoxic concentrations increased the frequency of DNA strand breaks in human primary skeletal muscle cells in multiple experiments in one study. WNiCo (91–6–3), but not WNiCo (97–2–1), increased the frequency of DNA strand breaks in a rat skeletal muscle cell line (L6-C11) in one study. Furthermore, sW/Ni/Co (92/5/3) induced DNA strand breaks and micronucleus formation in a human osteosarcoma cell line (HOS) in multiple experiments in two studies. No genotoxicity studies were available in non-human mammals in vivo or in non-mammalian systems.

Multiple lines of evidence suggest that WGTA induces oxidative stress. WNiCo (91–6–3) and WNiCo (97–2–1) increased levels of reactive oxygen species in rat L6-C11 cells, and in vitro exposure to sW/Ni/Co (92/5/3) increased levels of reactive oxygen species and reactive nitrogen species in rat pulmonary macrophages. Intraperitoneal injection of rats with sW/Ni/Co (91/5/4) caused increased levels of urinary metabolites indirectly associated with oxidative stress. Additionally, sW/Ni/Co (92/5/3) increased protein levels of FOS and NFKB1 (also known as NFκBRE) in a human cell line (HepG2).

WGTA-induced epigenetic alterations are suggested on the basis of histone modifications in vitro in two studies. Exposure to WNiCo (91–6–3) decreased phosphorylation of serine 3 on histone 3 in mouse primary neural cells and myoblast (C2C12) cells, and decreased acetylation of histone 3 in C2C12 cells. Trimethylation of lysine 4 on histone 3 was unaffected in either cell type. In rat L6-C11 cells, WNiCo (91–6–3) increased messenger RNA (mRNA) levels of histone methylase, histone acetylase, and histone deacetylase, while WNiCo (97–2–1) increased mRNA levels of histone deacetylase only. No in vitro or in vivo studies regarding other epigenetic changes were available.

Indirect evidence suggests that WGTA alters cell proliferation, cell death, or nutrient supply. Transcriptomic data from human primary skeletal muscle cells treated with WNiCo (91–6–3) and WNiCo (97–2–1), and from BALF cells collected from rats instilled intratracheally with sW/Ni/Co (92/5/3), showed changes in mRNA levels associated with anti-apoptosis, decreased wound healing, regulation of cell proliferation, differentiation, and altered cell growth arrest and senescence. WNiCo (91–6–3) and WNiCo (97–2–1) both decreased caspase 3 activity in rat cells, but not in human primary skeletal muscle cells, which is consistent with the gene expression changes indicating an anti-apoptotic effect. Altered nutrient supply was suggested on the basis of increased mRNA levels associated with glycolysis and angiogenesis in rat BALF cells, and changes in several metabolic pathways in the urine of rats injected intraperitoneally with sW/Ni/Co (91/5/4).

Indirect evidence suggests that WGTA is immunosuppressive. Thymus-to-body-weight ratio

Swas decreased in rats 3 months after intramuscular implantation of WNiCo (91–6–3). The phagocytic capacity of rat pulmonary macrophages was decreased by in vitro exposure to sW/Ni/Co (92/5/3). In addition, WNiCo (91–6–3) decreased mRNA levels of genes related to the immune response in human primary skeletal muscle cells.

WGTA caused immortalization, but only sW/Ni/Co was tested and not the alloy. Untreated immortalized HOS cells were non-tumourigenic in nude mice. However, HOS cells exposed to non-cytotoxic concentrations of sW/Ni/Co (92/5/3) for 24 hours became capable of anchorage-independent growth in soft agar and invasion into Matrigel, indicating neoplastic transformation. Injection of the transformed HOS cells into athymic nude mice caused adenocarcinomas, confirming that the cells were tumourigenic.

The effects of WGTA with regard to chronic inflammation are unclear. Studies with WNiCo (in rats) and sW/Ni/Co (in human cell lines and rats in vivo) showed evidence of pro-inflammatory responses, including increased peripheral neutrophils, lymphocytes, monocytes, and eosinophils in chronically exposed rats, but these findings are not necessarily associated with chronic tissue inflammation. Regarding the key characteristics "is electrophilic or can be metabolically activated to an electrophile", "alters DNA repair or causes genomic instability", or "modulates receptor-mediated effects", no data were available to the Working Group.

6. Evaluation and Rationale

6.1 Cancer in humans

There is *inadequate evidence* in humans regarding the carcinogenicity of weapons-grade tungsten (with nickel and cobalt) alloy.

6.2 Cancer in experimental animals

There is *sufficient evidence* in experimental animals for the carcinogenicity of weapons-grade tungsten (with nickel and cobalt) alloy.

6.3 Mechanistic evidence

There is *limited evidence* that weapons-grade tungsten (with nickel and cobalt) alloy exhibits key characteristics of carcinogens.

6.4 Overall evaluation

Weapons-grade tungsten (with nickel and cobalt) alloy is *possibly carcinogenic to humans (Group 2B)*.

6.5 Rationale

The Group 2B evaluation for weapons-grade tungsten (with nickel and cobalt) alloy is based on *sufficient evidence* for cancer in experimental animals. The *sufficient evidence* in experimental animals for the carcinogenicity of weapons-grade tungsten (with nickel and cobalt) alloy is based on an increase in the incidence of malignant neoplasms in two species. There is *limited evidence* in experimental systems that weapons-grade tungsten (with nickel and cobalt) alloy is genotoxic; causes epigenetic alterations; induces oxidative stress; is immunosuppressive; and alters cell proliferation, cell death, or nutrient supply. The evidence regarding cancer in humans is *inadequate* because no studies were available.

References

Adams VH, Dennis WE, Bannon DI (2015). Toxic and transcriptional responses of PC12 cells to soluble tungsten alloy surrogates. *Toxicol Rep*. 2:1437–44. doi:10.1016/j.toxrep.2015.09.005 PMID:28962486

ATSDR (2004). Toxicological profile for cobalt. Atlanta (GA), USA: Agency for Toxic Substances and Disease Registry. Available from: https://wwwn.cdc.gov/TSP/ToxProfiles/ToxProfiles.aspx?id=373&tid=64, accessed 22 November 2021.

ATSDR (2005a). Toxicological profile for tungsten. Atlanta (GA), USA: Agency for Toxic Substances and Disease Registry. Available from: https://www.atsdr.cdc.gov/ToxProfiles/tp186.pdf, accessed 22 November 2021.

ATSDR (2005b). Toxicological profile for nickel. Atlanta (GA), USA: Agency for Toxic Substances and Disease Registry. Available from: https://wwwn.cdc.gov/TSP/ToxProfiles/ToxProfiles.aspx?id=245&tid=44, accessed 22 November 2021.

Bardack S, Dalgard CL, Kalinich JF, Kasper CE (2014). Genotoxic changes to rodent cells exposed in vitro to tungsten, nickel, cobalt and iron. *Int J Environ Res Public Health*. 11(3):2922–40. doi:10.3390/ijerph110302922 PMID:24619124

Bednar AJ, Mirecki JE, Inouye LS, Winfield LE, Larson SL, Ringelberg DB (2007). The determination of tungsten, molybdenum, and phosphorus oxyanions by high performance liquid chromatography inductively coupled plasma mass spectrometery. *Talanta*. 72(5):1828–32. doi:10.1016/j.talanta.2007.02.016 PMID:19071839

Bostick BC, Sun J, Landis JD, Clausen JL (2018). Tungsten speciation and solubility in munitions-impacted soils. *Environ Sci Technol*. 52(3):1045–53. doi:10.1021/acs.est.7b05406 PMID:29307178

CDC (2018). Arsenic, chromium, and nickel in urine by ICP-MS. Method 3031.1-01. Revised 23 March 2018. Laboratory procedure manual. Atlanta (GA), USA: Centers for Disease Control and Prevention, United States Department of Health and Human Services. Available from: https://wwwn.cdc.gov/nchs/data/nhanes/2019-2020/labmethods/UTAS-UCM-UNI-K-MET-508.pdf, accessed 20 January 2022.

CDC (2019). Urine multi-element ICP-DRC-MS. Method 3018.6-06. Revised 28 February 2019. Laboratory procedure manual. Atlanta (GA), USA: Centers for Disease Control and Prevention, United States Department of Health and Human Services. Available from: https://wwwn.cdc.gov/nchs/data/nhanes/2017-2018/labmethods/UM-J-MET-508.pdf, accessed 20 January 2022.

Centeno JA, Rogers DA, van der Voet GB, Fornero E, Zhang L, Mullick FG, et al. (2014). Embedded fragments from U.S. military personnel—chemical analysis and potential health implications. *Int J Environ Res Public Health*. 11(2):1261–78. doi:10.3390/ijerph110201261 PMID:24464236

Clausen JL, Korte N (2009). Environmental fate of tungsten from military use. *Sci Total Environ*. 407(8):2887–93. doi:10.1016/j.scitotenv.2009.01.029 PMID:19217645

De Hauteclocque C, Morisset M, Kanny G, Kohler C, Mouget B, Moneret-Vautrin DA (2002). Asthme professionnel par hypersensibilité aux métaux durs. [Occupational asthma due to hard metals hypersensitivity]. *Rev Mal Respir*. 19(3):363–5. [French] PMID:12161703

Dinçer O, Pehlivanoğlu MK, Çalişkan NK, Karakaya İ, Kalkanli A (2015). Processing and microstructural characterization of liquid phase sintered tungsten–nickel–cobalt heavy alloys. *Int J Refract Met Hard Mater*. 50:106–12. doi:10.1016/j.ijrmhm.2014.12.009

Emond CA, Vergara VB, Lombardini ED, Mog SR, Kalinich JF (2015a). Induction of rhabdomyosarcoma by embedded military-grade tungsten/nickel/cobalt not by tungsten/nickel/iron in the B6C3F$_1$ mouse. *Int J Toxicol*. 34(1):44–54. doi:10.1177/1091581814565038 PMID:25544565

Emond CA, Vergara VB, Lombardini ED, Mog SR, Kalinich JF (2015b). The role of the component metals in the toxicity of military-grade tungsten alloy. *Toxics*. 3(4):499–514. doi:10.3390/toxics3040499 PMID:29051474

Gaitens JM, Centeno JA, Squibb KS, Condon M, McDiarmid MA (2016). Mobilization of metal from retained embedded fragments in a blast-injured Iraq war veteran. *Mil Med*. 181(6):e625–9. doi:10.7205/MILMED-D-15-00432 PMID:27244078

Gaitens JM, Condon M, Squibb KS, Centeno JA, McDiarmid MA (2017). Metal exposure in veterans with embedded fragments from war-related injuries: early findings from surveillance efforts. *J Occup Environ Med*. 59(11):1056–62. doi:10.1097/JOM.0000000000001119 PMID:28759480

Garrick MD, Dolan KG, Horbinski C, Ghio AJ, Higgins D, Porubcin M, et al. (2003). DMT1: a mammalian transporter for multiple metals. *Biometals*. 16(1):41–54. doi:10.1023/A:1020702213099 PMID:12572663

Gold K, Cheng YS, Holmes TD (2007). A quantitative analysis of aerosols inside an armored vehicle perforated by a kinetic energy penetrator containing tungsten, nickel, and cobalt. *Mil Med*. 172(4):393–8. doi:10.7205/MILMED.172.4.393 PMID:17484310

Gunasekar PG, Stanek LW (2011). Advances in exposure and toxicity assessment of particulate matter: an overview of presentations at the 2009 Toxicology and Risk Assessment Conference. *Toxicol Appl Pharmacol*. 254(2):141–4. doi:10.1016/j.taap.2010.10.020 PMID:21034760

Harris RM, Williams TD, Hodges NJ, Waring RH (2011). Reactive oxygen species and oxidative DNA damage mediate the cytotoxicity of tungsten–nickel–cobalt alloys in vitro. *Toxicol Appl Pharmacol*. 250(1):19–28. doi:10.1016/j.taap.2010.09.020 PMID:20934443

Harris RM, Williams TD, Waring RH, Hodges NJ (2015). Molecular basis of carcinogenicity of tungsten alloy particles. *Toxicol Appl Pharmacol*. 283(3):223–33. doi:10.1016/j.taap.2015.01.013 PMID:25620057

ICRP (1981). Metabolic data for tungsten. In: Limits for intakes of radionucleotides by workers. ICRP Publication 30 (Part 3). *Ann ICRP*, 6(2–3), 93–5. Available from: https://journals.sagepub.com/doi/pdf/10.1177/ANIB_6_2-3, accessed 8 August 2022. doi:10.1023/A:1020702213099

IFA (2022a). Tungsten and its compounds, soluble. Tungsten and its compounds, insoluble. GESTIS International Limit Values database. Germany: Institut für Arbeitsschutz der Deutschen Gesetzlichen Unfallversicherung (Institute for Occupational Safety and Health of the German Social Accident Insurance). Available from: https://www.dguv.de/ifa/gestis/gestis-internationale-grenzwerte-fuer-chemische-substanzen-limit-values-for-chemical-agents/index-2.jsp, accessed 9 February 2022.

IFA (2022b). Nickel, metal. Nickel, metal, total dust. Nickel, metal and compounds. Nickel compounds, insoluble. Nickel compounds, soluble. GESTIS International Limit Values database. Germany: Institut für Arbeitsschutz der Deutschen Gesetzlichen Unfallversicherung (Institute for Occupational Safety and Health of the German Social Accident Insurance). Available from: https://www.dguv.de/ifa/gestis/gestis-internationale-grenzwerte-fuer-chemische-substanzen-limit-values-for-chemical-agents/index-2.jsp, accessed 9 February 2022.

Kalinich JF, Emond CA, Dalton TK, Mog SR, Coleman GD, Kordell JE, et al. (2005). Embedded weapons-grade tungsten alloy shrapnel rapidly induces metastatic high-grade rhabdomyosarcomas in F344 rats. *Environ Health Perspect*. 113(6):729–34. doi:10.1289/ehp.7791 PMID:15929896

Kalinich JF, Kasper CE (2016). Are internalized metals a long-term health hazard for military veterans? *Public Health Rep*. 131(6):831–3. doi:10.1177/0033354916669324 PMID:28123230

Kalinich JF, Vergara VB, Emond CA (2008). Urinary and serum metal levels as indicators of embedded tungsten alloy fragments. *Mil Med*. 173(8):754–8. doi:10.7205/milmed.173.8.754 PMID:18751592

Kennedy KJ, Esmen NA, Buchanich JM, Zimmerman S, Sleeuwenhoek AJ, Marsh GM (2017). Mortality among hardmetal production workers: occupational exposures. *J Occup Environ Med*. 59(12):e297–305. doi:10.1097/JOM.0000000000001068 PMID:28704227

Lauvrak SU, Munthe E, Kresse SH, Stratford EW, Namløs HM, Meza-Zepeda LA, et al. (2013). Functional characterisation of osteosarcoma cell lines and identification of mRNAs and miRNAs associated with aggressive cancer phenotypes. *Br J Cancer*. 109(8):2228–36. doi:10.1038/bjc.2013.54924 PMID:24064976

Machado BI (2011). Ballistic projectile metallurgical issues and fundamentals: aerosol production in rod penetration erosion and erosion phenomena associated with railgun development [thesis]. El Paso (TX), USA. University of Texas at El Paso. Available from: https://scholarworks.utep.edu/open_etd/2331/, accessed 19 November 2021.

Machado BI, Murr LE, Suro RM, Gaytan SM, Ramirez DA, Garza KM, et al. (2010). Characterization and cytotoxic assessment of ballistic aerosol particulates for tungsten alloy penetrators into steel target plates. *Int J Environ Res Public Health*. 7(9):3313–31. doi:10.3390/ijerph7093313 PMID:20948926

Magness L, Schuster B, Weil S, Lavender C (2014). Demonstration of tungsten nanocomposite alternatives to depleted uranium in anti-armor penetrators. Final report. ESTCP Project WP-200805. Alexandria (VA), USA: Strategic Environmental Research and Development Program and Environmental Security Technology Certification Program. Available from: https://serdp-estcp.org/projects/details/b7ef21a4-41aa-4975-88c3-a3b77a243597, accessed 19 November 2021.

McInturf SM, Bekkedal MYV, Wilfong E, Arfsten D, Chapman G, Gunasekar PG (2011). The potential reproductive, neurobehavioral and systemic effects of soluble sodium tungstate exposure in Sprague-Dawley rats. *Toxicol Appl Pharmacol*. 254(2):133–7. doi:10.1016/j.taap.2010.04.021 PMID:21296100

McInturf SM, Bekkedal MYV, Wilfong E, Arfsten D, Gunasekar PG, Chapman GD (2008). Neurobehavioral effects of sodium tungstate exposure on rats and their progeny. *Neurotoxicol Teratol*. 30(6):455–61. doi:10.1016/j.ntt.2008.07.003 PMID:18675901

Michaux S (2021). Outlook for tungsten. Espoo, Finland: geological survey of Finland. Available from: https://tupa.gtk.fi/raportti/arkisto/2_2021.pdf, accessed 19 November 2021.

Miller AC, Brooks K, Smith J, Page N (2004). Effect of the militarily-relevant heavy metals, depleted uranium and heavy metal tungsten-alloy on gene expression in human liver carcinoma cells (HepG2). *Mol Cell Biochem*. 255(1–2):247–56. doi:10.1023/B:MCBI.0000007280.72510.96 PMID:14971665

Miller AC, Mog S, McKinney L, Luo L, Allen J, Xu J, et al. (2001). Neoplastic transformation of human osteoblast cells to the tumorigenic phenotype by heavy metal-tungsten alloy particles: induction of genotoxic effects. *Carcinogenesis*. 22(1):115–25. doi:10.1093/carcin/22.1.115 PMID:11159749

Miller AC, Xu J, Stewart M, Prasanna PG, Page N (2002). Potential late health effects of depleted uranium and tungsten used in armor-piercing munitions: comparison of neoplastic transformation and genotoxicity with the known carcinogen nickel. *Mil Med*.

167(Suppl 1):120–2. doi:10.1093/milmed/167.suppl_1.120 PMID:11873492

NIOSH (1994a). Tungsten (soluble and insoluble). Method 7074, Issue 2. In: NIOSH manual of analytical methods, 4th ed. Cincinnati (OH), USA: National Institute for Occupational Safety and Health. Available from: https://www.cdc.gov/niosh/docs/2003-154/pdfs/7074.pdf, accessed 20 January 2022.

NIOSH (1994b). Metals in urine. Method 8310, Issue 2. In: NIOSH manual of analytical methods, 4th ed. Cincinnati (OH), USA: National Institute for Occupational Safety and Health. Available from: https://www.cdc.gov/niosh/docs/2003-154/pdfs/8310.pdf, accessed 20 January 2022.

NIOSH (1994c). Elements in blood or tissue. Method 8005, Issue 2. In: NIOSH manual of analytical methods, 4th ed. Cincinnati (OH), USA: National Institute for Occupational Safety and Health. Available from: https://www.cdc.gov/niosh/docs/2003-154/pdfs/8005.pdf, accessed 20 January 2022.

Ogundipe A, Greenberg B, Braida W, Christodoulatos C, Dermatas D (2006). Morphological characterisation and spectroscopic studies of the corrosion behaviour of tungsten heavy alloys. *Corros Sci*. 48(10):3281–97. doi:10.1016/j.corsci.2005.12.004

OSHA (1994). Tungsten and cobalt in workplace atmospheres (ICP analysis). Method ID-213. Salt Lake City (UT), USA: Occupational Safety and Health Administration (OSHA), United States Department of Labor. Branch of Inorganic Methods Development. Available from: https://www.osha.gov/sites/default/files/methods/id-213.pdf, accessed 20 January 2022.

OSHA (2021). Tungsten, metal & insoluble compounds. OSHA Occupational Chemical Database. Washington (DC), USA: Occupational Safety and Health Administration. Available from: https://www.osha.gov/chemicaldata/524, accessed 17 February 2022.

Richardson JB, Dancy BCR, Horton CL, Lee YS, Madejczyk MS, Xu ZZ, et al. (2018). Exposure to toxic metals triggers unique responses from the rat gut microbiota. *Sci Rep*. 8(1):6578. doi:10.1038/s41598-018-24931-w PMID:29700420

Roedel EQ, Cafasso DE, Lee KW, Pierce LM (2012). Pulmonary toxicity after exposure to military-relevant heavy metal tungsten alloy particles. *Toxicol Appl Pharmacol*. 259(1):74–86. doi:10.1016/j.taap.2011.12.008 PMID:22198552

Sanghvi VR, Leibold J, Mina M, Mohan P, Berishaj M, Li Z, et al. (2019). The oncogenic action of NRF2 depends on de-glycation by fructosamine-3-kinase. *Cell*. 178(4):807–19.e21. doi:10.1016/j.cell.2019.07.031 PMID:31398338

Schuster BE, Roszell LE, Murr LE, Ramirez DA, Demaree JD, Klotz BR, et al. (2012). In vivo corrosion, tumor outcome, and microarray gene expression for two types of muscle-implanted tungsten alloys. *Toxicol Appl Pharmacol*. 265(1):128–38. doi:10.1016/j.taap.2012.08.025 PMID:22982072

Sheppard PR, Speakman RJ, Ridenour G, Glascock MD, Farris C, Witten ML (2007). Spatial patterns of tungsten and cobalt in surface dust of Fallon, Nevada. *Environ Geochem Health*. 29(5):405–12. doi:10.1007/s10653-007-9085-1 PMID:17345005

Shinn AM (2012). Cellular changes in response to embedded fragments: an animal surveillance model [dissertation]. Baltimore (MD), USA: University of Maryland, Baltimore. Available from: https://archive.hshsl.umaryland.edu/handle/10713/2305.

Sirri V, Leibovitch MP, Leibovitch SA (2003). Muscle regulatory factor MRF4 activates differentiation in rhabdomyosarcoma RD cells through a positive-acting C-terminal protein domain. *Oncogene*. 22(36):5658–66. doi:10.1038/sj.onc.1206690 PMID:12944914

Smith DE, Todorov T, Defante AP, Hoffman JF, Kalinich JF, Centeno JA (2021). Spectroscopic and spectrometric approaches for assessing the composition of embedded metals in tissues. *Appl Spectrosc*. 75(6):661–73. doi:10.1177/0003702820979748 PMID:33231488

Smith MT, Guyton KZ, Gibbons CF, Fritz JM, Portier CJ, Rusyn I, et al. (2016). Key characteristics of carcinogens as a basis for organizing data on mechanisms of carcinogenesis. *Environ Health Perspect*. 124(6):713–21. doi:10.1289/ehp.1509912 PMID:26600562

Smolders R, Schramm KW, Nickmilder M, Schoeters G (2009). Applicability of non-invasively collected matrices for human biomonitoring. *Environ Health*. 8(8). doi:10.1186/1476-069X-8-8

Sunwoo A, Groves S, Goto D, Hopkins H (2006). Effect of matrix alloy and cold swaging on micro-tensile properties of tungsten heavy alloys. *Mater Lett*. 60(3):321–5. doi:10.1016/j.matlet.2005.08.050

Tyagi R, Rana P, Gupta M, Bhatnagar D, Srivastava S, Roy R, et al. (2014). ^{1}H NMR spectroscopic analysis detects metabolic disturbances in rat urine on acute exposure to heavy metal tungsten alloy based metals salt. *Chem Biol Interact*. 211:20–8. doi:10.1016/j.cbi.2013.12.016 PMID:24412238

United States Geological Survey (1996). Tungsten. Mineral commodity summaries. Reston (VA), USA: United States Department of the Interior, United States Geological Survey. Available from: https://d9-wret.s3.us-west-2.amazonaws.com/assets/palladium/production/mineral-pubs/tungsten/tungsmcs96.pdf, accessed 27 January 2022.

United States Geological Survey (2021). Tungsten. Mineral commodity summaries. Reston (VA), USA: United States Department of the Interior, United States Geological Survey. Available from: https://pubs.usgs.gov/periodicals/mcs2021/mcs2021-tungsten.pdf, accessed 27 January 2022.

Upadhyaya A (2001). Processing strategy for consolidating tungsten heavy alloys for ordnance applications. *Mater Chem Phys*. 67(1–3):101–10. doi:10.1016/S0254-0584(00)00426-0

US EPA (1994). Method 200.8. Determination of trace elements in waters and wastes by inductively coupled plasma-mass spectrometry. Revision 5.4. EMMC Version. Cincinnati (OH), USA. Office of Research and Development, United States Environmental Protection Agency. Environmental Monitoring and Systems Laboratory. Available from: https://www.epa.gov/sites/default/files/2015-06/documents/epa-200.8.pdf, accessed 20 January 2022.

US EPA (1999a). Compendium method IO-3.2. Determination of metals in ambient particulate matter using atomic absorption (AA) spectroscopy. Cincinnati (OH), USA. Office of Research and Development, United States Environmental Protection Agency. Available from: https://www.epa.gov/sites/default/files/2019-11/documents/mthd-3-2.pdf, accessed 20 January 2022.

US EPA (1999b). Compendium method IO-3.4. Determination of metals in ambient particulate matter using inductively coupled plasma (ICP) spectroscopy. Cincinnati (OH), USA. Office of Research and Development, United States Environmental Protection Agency. Available from: https://www.epa.gov/sites/default/files/2015-07/documents/epa-io-3.4.pdf, accessed 20 January 2022.

US EPA (1999c). Compendium method IO-3.5. Determination of metals in ambient particulate matter using inductively coupled plasma/mass spectrometry (ICP/MS). Cincinnati (OH), USA. Office of Research and Development, United States Environmental Protection Agency. Available from: https://www.epa.gov/sites/default/files/2015-07/documents/epa-io-3.5.pdf, accessed 20 January 2022.

US EPA (1999d). Compendium method IO-3.1. Selection, preparation and extraction of filter material. Cincinnati (OH), USA. Office of Research and Development, United States Environmental Protection Agency. Available from: https://www.epa.gov/sites/default/files/2015-07/documents/epa-io-3.1.pdf, accessed 20 January 2022.

US EPA (2007). EPA SW-846 method 3051A. Microwave assisted acid digestion of sediments, sludges, soils, and oils. Cincinnati (OH), USA. Office of Research and Development, United States Environmental Protection Agency. Available from: https://www.epa.gov/sites/default/files/2015-12/documents/3051a.pdf, accessed 26 January 2022.

US EPA (2014). Inductively coupled plasma—mass spectrometry. Method 6020B. Revision 2. In: Test methods for evaluating solid waste: physical/chemical methods compendium (SW-846 Update V). Cincinnati (OH), USA: Office of Research and Development, United States Environmental Protection Agency. Available from: https://www.epa.gov/sites/default/files/2015-12/documents/6020b.pdf, accessed 20 January 2022.

US EPA (2015). Provisional peer-reviewed toxicity values for soluble tungsten compounds (various CASRNs). Report No. EPA/690/R-15/015F. Final. Cincinnati (OH), USA: United States Environmental Protection Agency. Available from: https://cfpub.epa.gov/ncea/pprtv/documents/Tungsten.pdf, accessed 27 July 2022.

US EPA (2017). Technical fact sheet – tungsten. EPA 505-F-17-004. Washington (DC), USA: Office of Land and Emergency Management, United States Environmental Protection Agency. Available from: https://www.epa.gov/sites/default/files/2017-10/documents/ffrro_ecfactsheet_tungsten_9-15-17_508.pdf, accessed 19 November 2021.

van der Voet GB, Todorov TI, Centeno JA, Jonas W, Ives J, Mullick FG (2007). Metals and health: a clinical toxicological perspective on tungsten and review of the literature. *Mil Med*. 172(9):1002–5. doi:10.7205/MILMED.172.9.1002 PMID:17937367

Vergara VB, Emond CA, Kalinich JF (2016). Tissue distribution patterns of solubilized metals from internalized tungsten alloy in the F344 rat. *AIMS Environ Sci*. 3(2):290–304. doi:10.3934/environsci.2016.2.290

Verma R, Xu X, Jaiswal MK, Olsen C, Mears D, Caretti G, et al. (2011). In vitro profiling of epigenetic modifications underlying heavy metal toxicity of tungsten-alloy and its components. *Toxicol Appl Pharmacol*. 253(3):178–87. doi:10.1016/j.taap.2011.04.002 PMID:21513724

Wasel O, Freeman JL (2018). Comparative assessment of tungsten toxicity in the absence or presence of other metals. *Toxics*. 6(4):66. doi:10.3390/toxics6040066 PMID:30423906

Wen AY, Sakamoto KM, Miller LS (2010). The role of the transcription factor CREB in immune function. *J Immunol*. 185(11):6413–9. doi:10.4049/jimmunol.1001829 PMID:21084670

Westberg H, Bryngelsson IL, Marsh G, Buchanich J, Zimmerman S, Kennedy K, et al. (2017). Mortality among hardmetal production workers: the Swedish cohort. *J Occup Environ Med*. 59(12):e263–74. doi:10.1097/JOM.0000000000001054 PMID:29215483

WHO (2000). Nickel. Chapter 6.10. Air quality guidelines for Europe, 2nd ed. Geneva, Switzerland: World Health Organization. Regional Office for Europe. Available from: https://www.euro.who.int/__data/assets/pdf_file/0014/123080/AQG2ndEd_6_10Nickel.pdf, accessed 27 July 2022.

Zoroddu MA, Medici S, Peana M, Nurchi VM, Lachowicz JI, Laulicht-Glick F, et al. (2018). Tungsten or wolfram: friend or foe? *Curr Med Chem*. 25(1):65–74. doi:10.2174/0929867324666170428105603 PMID:28464784